Wormlike micelles in green surfactant systems

Master's Thesis

By

Jaume Adrover Forteza

Department of Process and Life Science Engineering
Faculty of Engineering, LTH, Lund University
SE-221 00 Lund, Sweden

LUND UNIVERSITY

QUALITY BY UNDERSTANDING

2024

0. Abstract

α-Olefin Sulfonate surfactants offer a greener alternative to traditional sulphated surfactants thanks to their higher biodegradability. Their similar molecular structures should, in theory, allow them to be used in the same range of applications as the sulphonated counterpart. However, the newer alternative also comes with novel challenges. While the thickening of a formulation with a sulphated surfactant can be achieved by salt addition, novel sulphonated surfactants require the introduction of co-surfactants to the formulation. Previous studies at CR resulted in the design of a purification process that enhanced the viscosity build up capacity of the surfactant.

In this master thesis work, this purification method was applied and tested. Through techniques such as HPLC-MS and NMR the content of the surfactant was unveiled, revealing that the technical grade surfactant was a mixture of different compounds. Among them, the most possible culprit for hindering the thickening capacities were those holding an alcohol group in carbons distancing from the head group. Additionally, the surfactant-water system was further characterized utilizing SAXS and DLS, leading to the elaboration of a phase diagram. The acquired knowledge will help formulators incorporate the greener alternative in their products, and guide manufacturers on how to make a surfactant with enhanced properties.

1. Acknowledgements

Firstly, I would like to recognise the people working at Lund University that have helped me throughout the thesis. Always so kind, ready to lend their knowledge and time, giving your ins and outs on the project, and patiently teaching me how to use the equipment.

My deepest gratitude goes to CR Competence. Not only they have guided me through the completion of this thesis, but also made me feel part of the company. I can proudly say that, to a greater or lesser extent, I successfully bothered every single one of you with my questioning and query for help in multiple techniques. However, not even once I was declined that aid, and all of you were always ready to put your time and expertise to my disposal. I had never had such a fantastic time doing science, and your genuine curiosity has genuinely lit a fire inside me.

Finally, I would like to give an honourable mention to my main supervisor, Jonas, whose support, and counsel made this possible. Leading the way, but also pointing at me which literature and background I required, so I could do educated guesses and actively participate in the decisions making of the project.

To all and everyone involved, thank you.

Table of Contents

2. Aims and Motivation of the project

As humanity's concern for the environment grows, so does the need for "greener" alternatives. These are defined as products with less detrimental effects on the environment than their predecessors and, preferably, made from renewable sources. The chemical industry is no exception, and surfactants are a clear example of compounds on their way to make the green transition.

A client approached CR competence some time ago because they wanted to use α-Olefin Sulfonate (AOS) surfactant as an alternative to sulphated surfactants in their formulations. Because AOS is very similar to the widely used sulphated surfactants, e.g. sodium dodecyl sulphate (SDS), it could be theoretically used for the same applications. Not only that, but the greater biodegradability of AOS would help reduce the toll of their product on the environment. However, while the rheological properties of sulphated surfactants can be easily tailored by simply adding salt, formulators require the addition of cosurfactants like cocamidopropyl betaine (CAPB) to build up viscosity in technical grade AOS. CR, then, embarked on a project to characterize the technical grade AOS, and find out the explanation to the new challenges that AOS pose. Some interesting findings were achieved during said project, but the investigation was terminated before a complete understanding of AOS was achieved.

The aim of the thesis is to continue what started some years ago, and further characterize and tackle the problematics associated with the AOS surfactant. This project will contribute to the understanding of AOS, help formulators incorporate it into their products, and push the chemical industry towards a more sustainable future.

3. Introduction

3.1. Surfactants

The word “surfactant” is an abbreviation of surface-active agent. Surfactants are absorbed at the interface between two immiscible compounds, lowering the interfacial energy between the two. That is because the surfactant molecule contains two or more parts, some of which are soluble in polar solvents (hydrophilic group or head), while others in non-polar ones (hydrophobic group or tail.[1]

For any system, the limit of the lowering effect is reached once micelles start forming, and the surfactant monomer concentration becomes constant, the concentration at this point is referred as Critical Micellar Concentration (CMC). Micelles are, typically, spherical surfactant aggregates in which the soluble part of the molecule is in contact with the solvent, leaving the inner insoluble part pointing to the centre, out of reach of the surrounding phase. Micelles can act as a reservoir of surfactant molecules. Further increment in surfactant concentration does not reflect into a noticeable interfacial energy lowering, as the excess surfactant will either form new micelles or incorporate into existing ones. The latter, makes micelles grow, only in length and not in thickness, like in figure 1. This leads to micelles acquiring elongated shapes which can change the rheological properties of the solution, usually, increasing its viscosity. This is widely used, for example, in personal care products to obtain a better feeling or performance of the same.

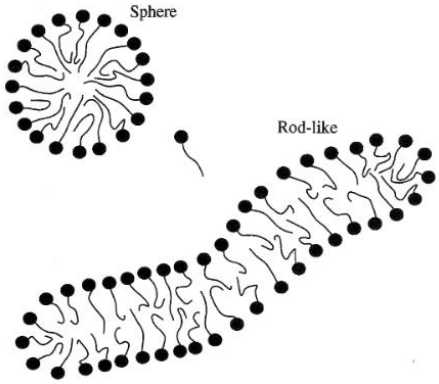

Figure 1: Illustration on micellar growth. Extracted from Kronberg, B., Holmberg, K., & Lindman, B. (2014b). Surface chemistry of surfactants and polymers. *John Wiley & Sons*.

The capacity of a surfactant to diminish interfacial energy is depending on the degree of packing of the surfactant at the interface, with greater packing implying a greater reduction. The characteristics of the head and the tail group, and especially their relative size to one another, will rule the ability of the surfactant to fit at the interface. One can estimate the packing efficiency using the Critical Packing Parameter (CPP) using equation 1, which additionally can be used to predict the phases that the surfactant of interest can give rise to, figure 2. However, the CPP must be taken with a grain of salt since it only takes into account the surfactant-water system, when, in the majority of formulations, salts, co-surfactants and other surfactants are habitually present, altering the packing. [2]

$$CPP = \frac{V}{A * l}$$

Equation 1: CPP equation where V is the volume of the tail, A area of the head and l represents tail length.

Depending on the packing and the surfactant concentration, different phases rise from the self-assembly of surfactant molecules, see figure 2 A and 2 B. Just like elongated micelles, the presence of these structures affects the solution's rheological properties. Given the right conditions, it is also common to find more than one structure co-existing in a system. Note that the characteristics of the surfactant might favour or forbid the presence of a certain structure, but it can, again, be altered to some extent by the presence of co-surfactants, electrolytes, or other surfactants.[3]

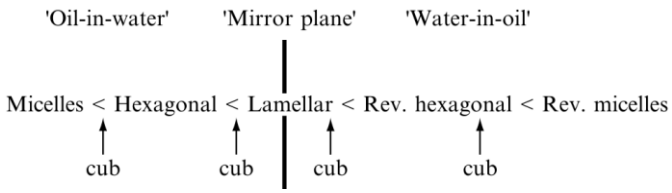

Figure 2A: Fontell scheme relating concentration of surfactant to the phases. Extracted from K. Fontell, Colloid Polym. Sci., 268 (1990) 264.

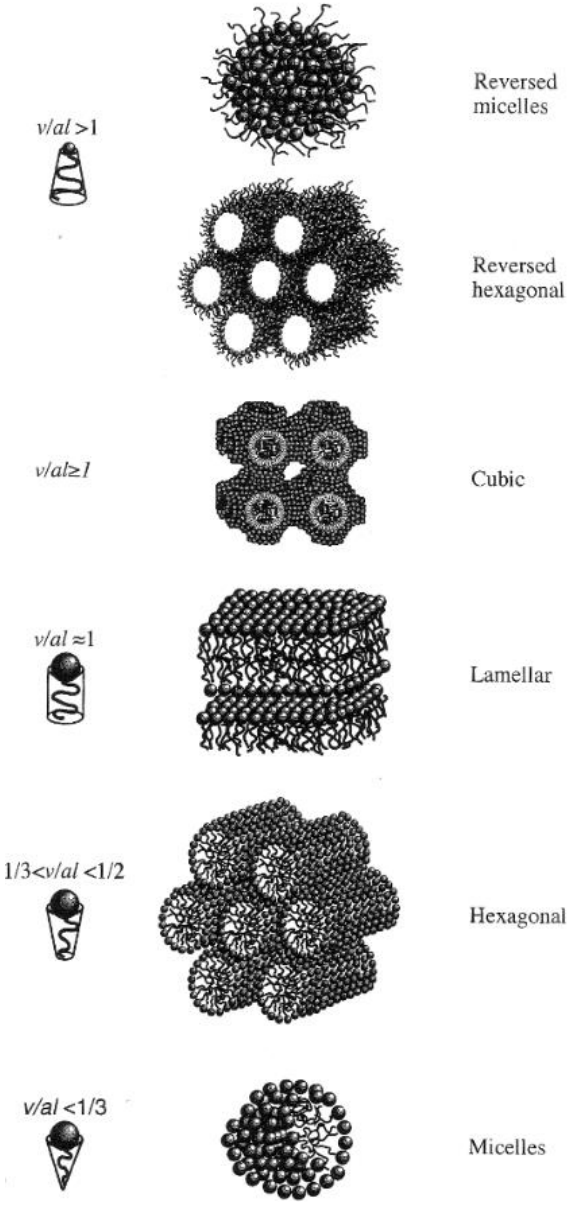

Figure 2 B: Typical surfactant structures related to their critical packing parameter. Extracted from Kronberg, B., Holmberg, K., & Lindman, B. (2014b). Surface chemistry of surfactants and polymers. *John Wiley & Sons*.

Another important factor is the temperature's effect on the surfactant self-assembly. Many ionic surfactants present a heavily temperature-dependent solubility. The solubility of a said surfactant can be extremely low at a set temperature and then increase drastically by orders of magnitude with a slight temperature increase. This phenomenon is addressed as Krafft point and it has a great influence on the viability of surfactants in practical applications.

3.2. AOS

Surfactants are classified by their polar groups charge. Anionic surfactants have a negatively charged head, cationic surfactants a positively charged one, zwitterionic have a both charges, and non-ionic do not have any. AOS falls into the anionic surfactant class because its head group consists of a sulfonate with a negative charge, see figure 3. Anionic surfactants are the largest surfactant class and the most widely used. Although they are generally sensitive to hard water, sulphonated surfactants show great resilience to it, and are stable at wide pH ranges. Additionally, AOS surfactants are considered mild in terms of safety, and have higher biodegradability than sulphates.

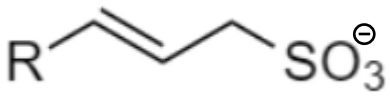

Figure 3: Molecular structure of AOS, where R is an aliphatic carbon chain. The sum of all the carbons is either 14 or 16.

3.3. The previous project at CR Competence

The previous project at CR Competence revolved around the characterization of polymer-surfactant systems. During the time, multiple surfactants were tested, and some interesting findings were made in the technical grade AOS. It was thought that AOS could not give rise to micellar growth by simple salt addition, but research showed otherwise. Formulations with additional salt, and with salt and 1-dodecanol showed a viscosity increase, and more experiments focusing on the rheological properties of different surfactant systems were done.

In those, although there were some good results, many samples either showed no viscosity increase, or phase separated, which was not desired. It was also hypothesized that the reason behind the mixed result were impurities contained in the technical grade AOS.

In an attempt to get rid of the salt excess, a purification process using methanol was employed. Then, the same experiment was performed with the new purified AOS samples and better results were obtained. This proved that the purification process was successful to some extent, and that it had removed all or part of the culprit.

Among the conclusions drawn, it is important to mention the limits for the surfactant to salt ratio and the dodecanol concentration. Regardless of the AOS used, all samples exceeding a 10:3 weight per cent ratio of surfactant to salt phase separated, and the same happened in formulas with over 1% in weight of 1-dodecanol. Nevertheless, a sweet spot was achieved in formulations with 15:2:1 and 15:3:0, with those numbers implying surfactant,

NaCl and 1-dodecanol weight percent, respectively. In those, a great increase in viscosity was obtained while maintaining a clear solution. These samples also showed shear-induced birefringence.

Afterwards, the purified and unpurified AOS were analysed using HPLC-ELS (High Performance Liquid Chromatography – Evaporative Light Scattering). The chromatograms, shown in figure 4, indicated the presence of multiple compounds in the AOS. Characterization of the peaks was not possible due to the lack of standards, but it supported the hypothesis of impurities hindering micellar growth.

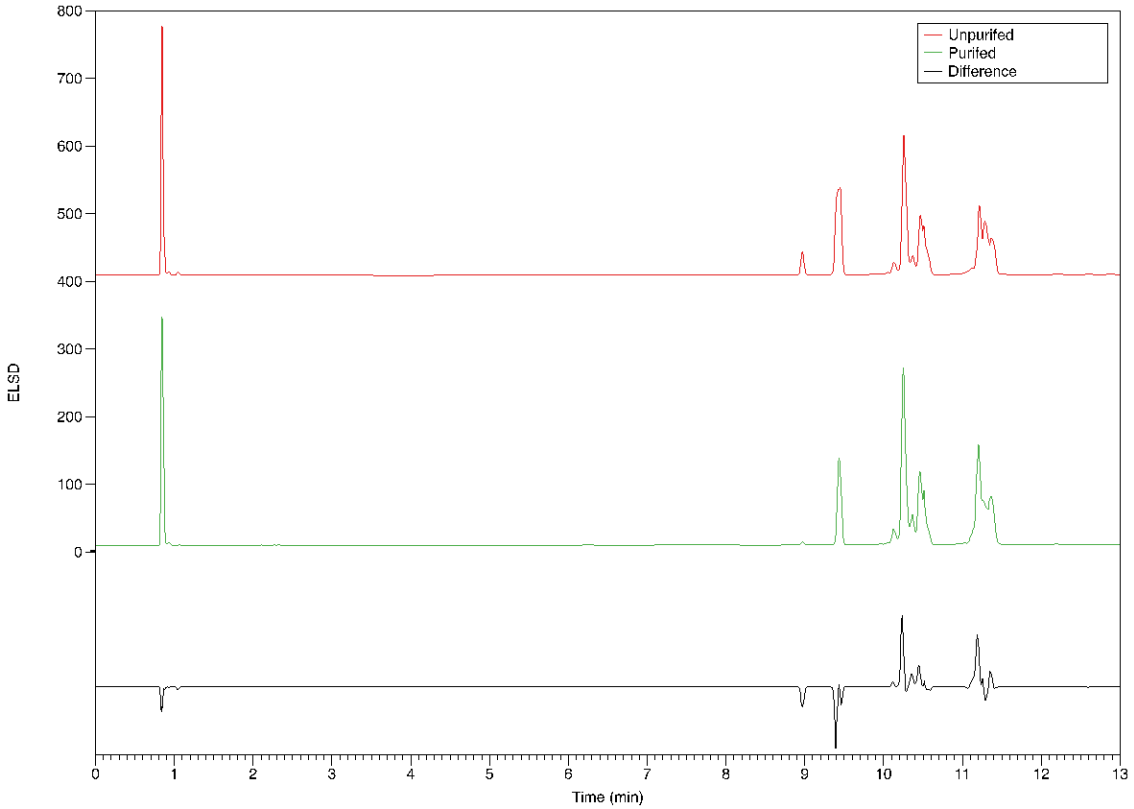

Figure 4: HPLC-ELS chromatograms from purified and unpurified AOS, and their difference. Extracted from the previous project at CR Competence.

3.4. Understanding the root of the problem

It was concluded in the previous project that impurities were the most possible responsible for the micellar growth hindrance. The next step would be, of course, to find out what those were. For that, the synthetic route of AOS was studied.

Although there are ways to produce AOS from renewable sources, nowadays, most of it still derives from petrochemicals. A scheme of the AOS synthetic process from petrochemicals is shown in figure 5. The main ingredients for its synthesis are α-Olefins and sulphur oxide (SO_3), and these two can come with their own collection of impurities. α-Olefins, obtained typically from a Ziegler[4], modified Ziegler or SHOP[5] process, include a variety of carbon chain lengths, and could retain traces of the catalytic reagents. SO_3's production also involves by-products such as sulphurous acid (H_2SO_3), and its own number of catalytic reagents. Upon reaction, α-Olefins and SO_3 form a sultone ring, which is then cleaved using sodium hydroxide (NaOH). However, along with the final AOS product, the treatment with

NaOH can give rise to other sultones and to non-desired hydroxy by-products.[6] With that in mind, a first outline for the project was elaborated to include techniques that could reveal information about the ions, isomers of the surfactant, and by-products present in the technical grade AOS.

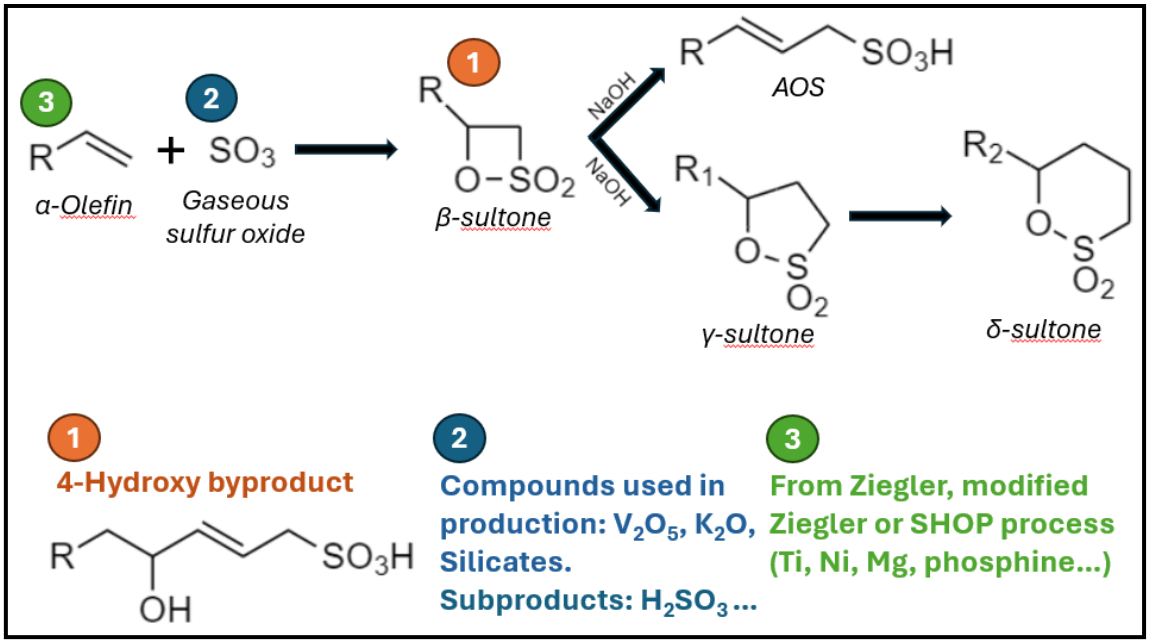

Figure 5: Synthetic scheme of AOS and its respective impurities and by-products.

4. Experimental Background

4.1. Birefringence

An easy, fast, and inexpensive way to check if there is micellar growth in a sample is looking at it through two crossed polarizers, against a light source. If there is an anisotropic construct in the sample, light will go through both polarizers, if there isn't, no light should shine through. A scheme of the technique is found in figure 6.

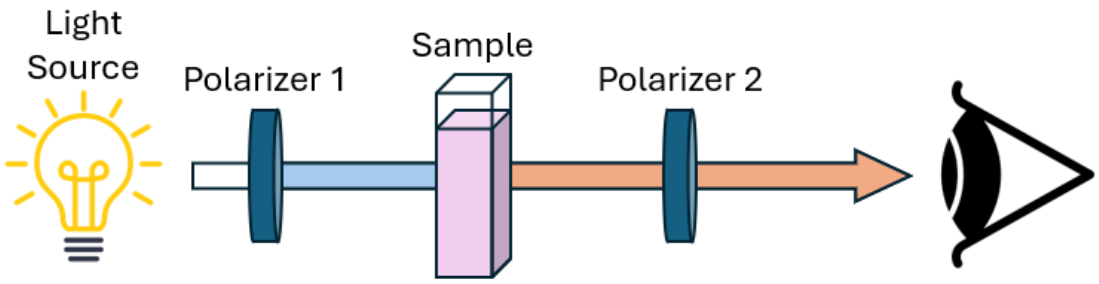

Figure 6: Birefringence experiment set up.

The three possible outcomes when analysing a sample are:

- No light gets through, independently of applying an external stress, the sample is not anisotropic.
- Light goes through without applying an external stress, implying the sample is anisotropic.
- Light goes through, but only when an external shear stress is applied.

The last case implies the presence of anisotropic particles, but they are randomly directed in solution when there is no shear stress, which prevents almost all light to get through. However, they arrange with the flow once an external stress is applied, redirecting the polarized light, and allowing it to cross the second polarizer. This is the typical behaviour of a sample with elongated micelles.

4.2. Viscosity

Shortly, viscosity can be viewed as the resistance of a fluid to deformation upon application of an external stress. It is one of the most important properties in, among others, cosmetics, food, and pharmaceuticals products as it impacts greatly on the sensory profile. Moreover, it influences their stability, packing and production. Surfactant have historically been used to tailor the viscosity of goods, and understanding how to manipulate AOS to tailor viscosity is essential to push its use in the market.

Visual inspection can be used to compare the viscosity of samples to a certain extent. However, using a rheometer gives much more reliable and sensitive results.[7]

4.3. Surface tension

Surface tension plays an important role in phenomena such as wetting, droplet formation, emulsions, and foams. Therefore, its understanding and characterization is relevant to unveil the potential of AOS and compare it to other surfactants on the market.

A liquid's surface tension can be measured by gently stretching its surface until it ruptures. The higher energy one has to put into it, the higher the surface tension is. An elevated surface tension is an indicator for how much the liquid molecules prefer to interact between themselves rather than with the surrounding media (usually air). As stated before, once the surface tension value reaches its minimum the CMC is reached.

4.4. HPLC

HPLC is an analytical technique used to separate analytes of a mixture based on their different capacity to adsorb from an adsorbent material. In that, a pump is used to inject the sample into a system where it will be carried by a media referred as "mobile phase". This mobile phase will take the analytes to an adsorbent material, or stationary phase, typically a packed column with a functionalized resin or silica inside. Depending on how the analyte interacts with both phases, it will be eluted at one time or another, leading to the separation of the components of the mixture.

HPLC, as it is, is used for analysis in a variety of processes and industries, but it also can be complemented with multiple kinds of detectors to perform continuous analysis on eluting species. Overall, HPLC has become one of the most widely employed analytical techniques in the chemical industry and in academic research.

4.4.1. ELS

In HPLC-ELS, the eluted solution by an HPLC instrument is mixed with a carrier gas (usually N_2) and nebulized into a thin mist. The newly formed droplets are conducted through a heated drift tube that evaporates the mobile phase, leaving the particle of the analyte dry. Finally, the particles are carried to the ELS detector region where they cross a beam of light, scattering it. The scattered light is detected, and an intensity signal is registered creating the chromatogram.

4.4.2. MS and MS/MS

Mass spectrometry (MS) is a powerful analytical technique that allows for the detection of the molar masses of a wide variety of molecules with great sensitivity and accuracy. In general words, the sample is fed into the equipment and an ionization source breaks the molecules apart forming charged fragments. These fragments will be separated depending on their charge and mass by a mass analyser capable of discerning the mass of the molecule.[8]

The ionization source selected was Electrospray Ionization (ESI) because it was in-house available, and it can easily be adapted into HPLC, allowing for the characterization of the individual peaks in a chromatogram.

In ESI, a fine spray of charged droplets is created as the solution is pushed through a charged needle-like capillary. This needle transfers its charge into the solution, generating droplets of the same polarity. Now, the droplets are transported to the mass analyser thanks to a potential and pressure gradient. During their transport, the droplets are shrunk through solvent evaporation by exposure to a stream of nitrogen. This process increases the charge density at the surface of the droplets until the combination of the electrical field and the charge density reaches a critical point and the ions at the surface are ejected and move into a gaseous phase. Finally, the ions are skimmed through a cone and accelerated into the mass analyser for their analysis.[9] With AOS containing a permanently charged sulphonate group, the ionization conditions could be kept to mild levels.

The selected mass analyser was a linear ion trap because it was readily available, compatible with ESI, and could perform tandem mass spectrometry (MS/MS). A linear ion trap, or quadrupole linear ion trap, can contain or eject ions to the detector by adjusting the radio frequency at which they are exposed. Ions are ejected based on their mass to charge ratio. If a determined frequency gives a signal on the detector, assuming the charge of the molecule, the mass of the ejected molecule can be known.

Once the mass of the molecule is known, then is up to the chemist to solve the puzzle and find the right combination of atoms that give rise to that number. Luckily, in this project, there was a preconceived idea of what those molecules would look like, making this task much easier.

4.5. SAXS

Small Angle X-Ray Scattering, or SAXS for short, is a technique reliant on the shape as well as the relative distances between particles or structures. The X-Ray beam is directed at the sample and some of it is scattered and then collected in the detector. In SAXS, the intensity of the signal (I) and the scattering vector (Q), which relates the angle difference between the inciting beam and the scattered one, are registered. The more intense a signal is, the more prominent the same distance is in the sample. SAXS is used to find the distance between structures, and to characterize those same structures. The latter being possible thanks to the scattering interference following Bragg's law.[10]

4.6. NMR

Nuclear magnetic resonance (NMR) is used to resolve the structure of molecules, their motions, and to study the self-assembling structures present in a sample. In this case, it was used to resolve the structure of the molecules that were present in AOS, especially isomers.[11]

NMR utilizes the magnetic momentum (μ) raised from the spin of an atom's nuclei to study its surroundings. For nuclei with spins of $I = ½$, the further analysis is fairly straightforward. An NMR experiment consists of applying an external magnetic field (B_0), which will force μ to orient parallelly or antiparallelly to it, see figure 7 below.

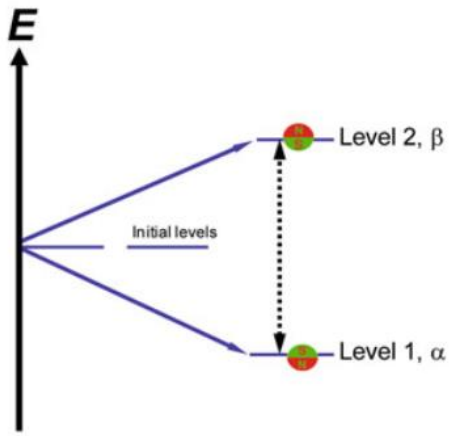

Figure 7: Representation of the energy level split after applying an external magnetic field on a nuclei.

This causes a precession on the spin whose angular frequency can be defined as:

$$w = 2\pi\nu$$

Equation 2.

And:

$$w = \gamma \cdot B_0$$

Equation 3.

Where ν is the frequency and γ represents the gyromagnetic ratio, specific for each isotope.

Because the parallel and antiparallel states have slightly different energies, an imbalance in their populations appears. However, if the right energy is applied, a nucleus can move from the lowest energy state (α) to the highest (β) until an equilibrium is met. This absorbed frequency gives rise to the registered signal.

In this project, proton-NMR (^{1}H-NMR) and ^{13}carbon-NMR (^{13}C-NMR) were used. Each absorb at different radiofrequencies and provide equally valuable information. ^{1}H-NMR exposes the environment and characteristics of the hydrogen atoms in the sample (with solely one proton in their nucleus). ^{13}C-NMR provides information about the chemical environment of the carbons in the molecule.

In ^{1}H-NMR, neighbouring protons make the signal split, creating multiplicity. When B_0 is applied and a hydrogen (H_A) aligns with it, it can result in a parallel or antiparallel alignment, generating two new, slightly different magnetic (B_{0A} and B_{0B}) fields. These new fields are felt by the neighbouring hydrogen bond to the next carbon (H_B). Depending on which alignment H_A has taken, H_B will generate the signal corresponding to either B_{0A} or B_{0B}. Due to the population of these two states being very similar, the intensity of the two peaks will also be very similar. With the same mechanism, two adjacent protons will split the signal into a triplet, and three protons to four. For three and four peaks, the inner peaks have higher intensity thanks to two new B_0 being extremely close. The final number of peaks in the spectra is equal to the number of neighbouring hydrogens plus one (N+1).

^{13}C-NMR also has splitting due to the neighbouring hydrogens. While this provides useful information in ^{1}H-NMR, in ^{13}C-NMR it tends to make spectra messy due to the lower

sensitivity of the technique. Fortunately, a decoupling method can be used to blend the signals coming from the same carbon into one.[12]

The other variable parameter of a nuclei in the NMR spectra is the radio frequency at which it absorbs. Depending on the neighbouring functional groups, the absorption happens at higher or lower energies. This effect is called chemical shift, and it is used to determine the neighbouring chemical groups to the studied nuclei. The chemical shift is a very studied and known phenomenon, and many books and articles include table or schemes that aid in the recognition of said groups and the overall molecule structure.

4.7. DLS

Dynamic Lights Scattering (DLS) measures the diffusion of the particles and translates that into a hydrodynamic radius (R_H) of a model sphere. For optimal results, the particles' diffusion should be mostly governed by Brownian motion. For charged particles, the diffusion will partly be influenced by electrostatic repulsions, leading to an apparent diminish in R_H. Since AOS has a charged head group, so will be the case in this project.

Simplistically, the experiment consists of passing a laser beam through the sample, where the particles in the solution will scatter the beam in all directions. A detector, set at a certain angle from the inciting beam, will register the scattered light at time "t". Then, another measurement is made very shortly after "t+1", and so on. The registered images are compared to the first one to find correlation. The closer in time the images were taken to the original, the larger the correlation will be. Then, the correlation is plotted against time. The shape of the function is dependent on how fast the particles are diffusing. Following the Stokes-Einstein equation, equation 4, larger particles will diffuse slowly while smaller ones will do it faster, leading to a much faster decay in correlation[13]:

$$D = \frac{k_B T}{6\pi\eta r}$$

Equation 4. Stokes-Einstein equation.

Where D is the diffusion coefficient, k_B is the Boltzmann constant, T is the temperature in Kelvin, η stands for the dynamic viscosity of the fluid, and r is the diameter of the particle, equivalent to R_H in our case.

The resulting correlation function is used to elaborate a size distribution against intensity plot. The latter plot can be transformed into a volume, and thereafter, a number distribution using Mie theory. However, that is not advised, as it implies using models which may differ from the sample's reality, giving rise to errors.

The resulting sizes are, again, of an equivalent sphere used as model. The elongation of the micelles must be calculated afterwards. This process is facilitated by the previous SAXS performed, that already exposed the length of the short axis radii of the micelles. Also, when presenting the results, it is appreciated to convert the acquired value of R_H to the diffusion parameter "D", found in equation 4.

Comparing different concentrations of purified and unpurified AOS samples will enlighten how different the growth for the two systems.

5. Methods

5.1. Sample preparation

5.1.1. Unpurified AOS

The commercial technical grade AOS comes as a 40% mass aqueous solution. But having it as a dry powder would ease its manipulation and further conduction of experiments. So, accordingly, the first step was drying the mother solution. A rotating evaporator was the equipment of choice since it allowed for a fast drying at low temperatures that would not degrade the sample. The instrument combines an oven with 3 different powers, those being low, medium, and high, with a vacuum pump and a rotating plate with a single speed.

With the equipment placed in the fume hood, the plate is loaded with test tubes filled up to half capacity of the technical grade AOS solution. Then, the evaporator is shut, the rotator started, the oven is set at medium, and the pressure decreased using the vacuum. Roughly, every 30 minutes to 1 hour the drying must be stopped because the dried surfactant forms a layer on top of the tubes, preventing further evaporation. The film will, eventually, become the sample used in the experiment, therefore, it must be removed from the tube and stored. This is repeated until no more sample is left inside the tubes.

The collected sample is not completely dry yet, it must be grinded and left drying in the fume food until a dry, free-flowing powder is achieved. Finally, the dried surfactant is transferred into its final container and labelled. Since this sample was obtained merely through desiccation, it will be used as reference or control, and addressed as unpurified (U or UP) AOS.

5.1.2. New Purified AOS

Since the previous purification method conducted during the previous CR Competence project gave rise to a better performing of AOS, the same method was used in the thesis. The reason being that understanding the difference in composition between the two versions of AOS will shine light on what is causing the issues.

The purification or purification method consists of mixing 1.5 L of the commercial technical grade AOS with 0.5 L of deionised water and 2 L of methanol, and then mixing. Afterwards, the mixture is left to rest for 24 hours, allowing for a precipitate to form. Then, the mixture is filtered using a Kitasato flask, Büchner funnel, filtering paper and a pump to create vacuum, like in figure 8. Afterwards, the collected precipitate is left to dry in the fume hood, then milled and left to dry again. This process is repeated until a dry, free-flowing powder is achieved. The AOS obtained in this form is addressed as new purified (NP).

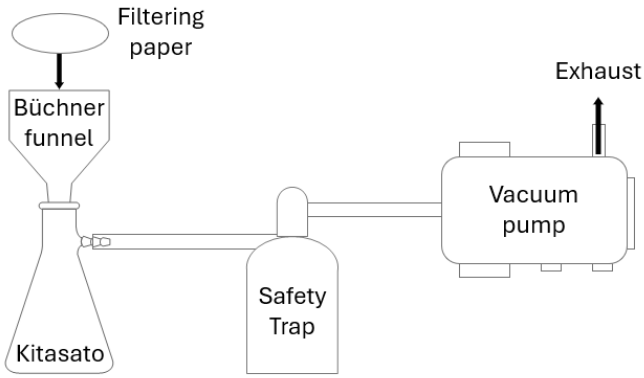

Figure 8: Vacuum filtering set up.

5.1.3. Old Purified AOS

The AOS that was purified at CR Competence during the original project is used as control against the NP AOS to ensure the reproducibility of the process and the achievement of a similar product. It is readily available and in powder form, and it is addressed as old purified (OP) AOS.

5.1.4. Second filtration AOS

The remaining liquid after the filtration was left to rest and new precipitate had formed. That precipitate was also filtered and dried for later studies.

5.1.5. Left over AOS

The remaining liquid after the second filtration process could potentially present useful information and is, therefore, collected. Then, it undergoes the same drying process as UP AOS and labelled as liquid (L) AOS.

5.1.6. Other Surfactants

Two other sulphonated surfactants were treated in the same manner as AOS, with the only difference that they were available in powder form from the start. Both, namely, sodium cocoyl isethionate (SCI) and sodium methyl cocoyl taurate (SMCT), possess similar potential to AOS, but also unresolved challenges. Performing the same purification process onto them could, like in AOS, result in a new product with enhanced properties.

5.2. Birefringence

Similarly to what had been done in the previous project, a number of samples were prepared to study the impact of sodium chloride (NaCl) and 1-dodecanol on the different versions of AOS. The samples used can be found in table 4.

After the source of light in the instrument is lit, the samples are introduced manually between the two polarizers. If no light reaches the observer's eye, then the samples are shaken on the spot and checked again.

5.3. Viscosity, visual inspection

The same samples tested for birefringence, shown in table 4, were used in the visual viscosity test. In that, the samples were compared to deionized water and to an old sample made in the previous CR Competence project. The comparison with plain water allowed to easily tell if an increase in viscosity occurred, while comparing it to the old sample works as a fast reproducibility check. The old sample of choice was made using 15% mass of treated AOS, 3% mass of NaCl and no 1-dodecanol, and showed a moderate increase in viscosity.

5.4. Surface tension and CMC experiment

Both, the surface tension and the CMC can be determined employing an analogue tensiometer. An apparatus consisting of a level adjusting base, a torsion wire, a reading plate, a calibration panel, a measuring platform, and a metal ring, see figure 9 below.

Figure 9: Analogue tensiometer. Image extracted from cromocol.se.

To setup the experiment, firstly, the base is levelled out, ensuring that the whole experiment will be performed on a flat surface without inclination. Secondly, the torsion wire is adjusted to mark 0 on the reading plate. Then, the recipient holding the study liquid is put onto the measuring platform. The metal ring is now cleaned and hanged from the hook connected to the torsion wire by the small hole in the thinner end of the piece. The measuring platform and the torsion wire are adjusted so that the ring is sitting underneath the liquid-air interface, the tension reading is 0, and the holder of ring is set properly in the calibration panel above, well into the white zone, between the two black zones on the panel.

During the experiment, the torsion wire is turned right, increasing its tension and the number on the reading plate. That makes the ring to step outside of the calibration panel and the measuring platform must be adjusted at the same time to ensure that the ring is kept within its bounds. The tension and platform are adjusted until the surface tension of the liquid is surpassed and the ring leaves the sample. The number on the reading plate will equal the surface tension of the liquid. Doing replicas is recommended.

The protocol for cleaning the ring consists of gently applying water and then ethanol onto it. Afterwards, eliminate all possible residues by exposing it to a flame while constantly and rapidly rotating the ring to avoid heat deformation. The ring must be cleaned before the first measurement, every time the measured sample is changed, and before storing it in its case. The ring is the most sensitive part of the instrument, and shall be handled with care, never put pressure on the metal ring and always hold it by its other end.

5.5. HPLC-ELS experiments

5.5.1. Pharmaceutical column

Addressed as pharmaceutical column, its commercial name is "Acclaim Trinity P2 Column", a product from Thermo Scientific™. The column is designed for counter-ion assay mainly, which makes it a great choice to analyse the salts contained in the AOS samples, and how it changes after the purification process. The column's dimensions are 3.0 x 100 mm and its filling has a particle size of 3 µm.

The mobile phase utilized was Mili-Q water and Mili-Q water with 0.1 M ammonium formate, adjusted to pH 3.65. After purging the system and conditioning the column, the flow was set to 0.600 mL/min and a ramp in the mixture of mobile phase programmed as in table 1:

Table 1: Mobile phase ramp for the counter-ion experiment. The proportion is linearly shifted over the interval of time given.

Time (min)	Volume % of Mili-Q Water	Volume % of Water with ammonium formate
1.00	90	10
9.00	0	100
15.00	0	100
15.01	90	10
23.00	90	10

The five different AOS samples mentioned before were used to prepare five solutions at 1% mass using Milli-Q water, plus two standard solutions of salt, were tested using this method. As on a first approach quantification was not of interest, two standards to locate the peaks of the counter-ions in the chromatogram were enough.

5.5.2. Surfactant Column

The Acclaim Surfactant Plus column, or surfactant column for short, is also a product from Thermo Scientific™. This column is designed to determine the different kinds of surfactants included in goods such as pharmaceuticals, food, and soaps. Therefore, it is a powerful tool

to analyse the present molecules in our surfactant system. Fortunately, or unfortunately, salts are eluted within the first minutes of elution in bulk, they cannot be characterized, but this allows the column to be easily used in mass spectrometry experiments.

The columns dimensions are 3.0 x 100 mm filled with 3 µm particles. The mobile phases used were Mili-Q water solution with 0.1 M ammonium acetate adjusted at pH 5.2, and HPLC grade acetonitrile. After purging the system and conditioning the column, the flow was set at 0.6 mL/min and a mobile phase set as in table 2:

Table 2: Mobile phase ramp for the surfactant column.

Time (min)	Volume % of Mili-Q Water	Volume % of Water with ammonium formate
1.00	80	20
13.00	15	85
13.01	80	20
16.00	90	20

The five different kinds of AOS were prepared in the same manner as for the previous column, but no standards or references were used to identify the peaks due to the lack of available pure compounds. Only a NaCl solution was tested to verify the elution of the salts at the beginning of the chromatogram.

5.6. HPLC-MS and MS/MS experiment

The usage of the HPLC-MS was allowed as a collaboration between the Physical Chemistry department and the Division of Biotechnology, Department of Chemistry in Lund. The HPLC-MS and MS/MS was performed using the same surfactant column and parameters as in HPLC-ELS. And, again, all five versions of AOS were analysed, and no standards used.

After an initial run of regular MS, multiple scans for just a certain mass were done to elaborate the eluting profile of individual species. Finally, MS/MS was performed to investigate the fragmentation patterns of the present molecules.

5.7. The SAXS experiment

5.7.1. SAXS' data collection

The SAXS instrument used was the Ganesha 300XL – Pinhole SAXS system, by SAXSLab. The SAXS was used two times to analyse a total of 22 samples. On the first set, 10 samples containing a mix of representants of the birefringence experiment were used in combination with some old birefringent samples made during the previous CR project. The next run consisted of 12 samples taken from the phase diagram experiment.

Depending on the sample's viscosity, two sampling methods can be employed. For the most viscous ones, a "sandwich" sample cell is preferred where the sample is pressed between two mica glasses and sheets in a metal piece. The more liquid-like are introduced with a pipette in a thin capillary tube held by a metal cover. The samples are introduced into the

holder inside the equipment and the door shut. Then, through some commands, the air inside the equipment is evacuated to almost zero and the measurement can be started.

The scale at which the equipment can registering signal has three possible configurations. Each of them is suited best to collect distinct q range or repeat distance. The higher the q value, the shorter the distance and the less time is necessary to collect data. As we move to longer distances, the collection time increases. For the shortest configuration a few minutes are enough to obtain detailed data, but longer distances will take hours.

A first wide scan is done to narrow down the configurations with relevant information, and then, the whole experiment is performed on those configurations to avoid an excessive time loss. For the sake of time, a computer script was made and run to automate the data collection once the samples were fed into the machine.

5.7.2. SAXS' data treatment

Once the data was collected, the files were transferred into a personal computer. Subsequently, the data was loaded into Primus, a program for SAXS data treatment. There, the different configurations registered for a single sample were merged into one, avoiding excessing overlaying between the configurations, and eliminating the error that rises from the data collection close to the q limits in a configuration. Finally, water signal is subtracted from the merged files.

The resulting data is taken into SasView. There, the user can visualize the data and draw a model structure on top of it. This model can be adjusted by changing the parameters on a window next to it. The objective would be to get the model to be as close as possible to the reality of the data, leading to the parameters being the actual characteristics of the system and solving the analysed structure.

5.8. The NMR experiment

One unpurified and another purified solution of AOS were prepared, both with 50 mM concentration. The solvent of choice was deuterated water (D_2O) to avoid, or at least reduce, the water signal. Then, 0.6 mL of the solutions were transferred into NMR tubes for analysis.

Both ^{1}H-NMR and ^{13}C-NMR spectra were collected on the instrument avance500, with 500 MHz. In ^{1}H-NMR, the water suppression was enabled, pulse width used of 11.8 and 22.0 µs. Sweep width was 10.000 Hz, acquisition time 3 second, and number of scans 8. For the ^{13}C-NMR the parameters were: 1 second acquisition time, number of scans 1028, sweep width 29760 Hz, and pulse width of 9.2 to 95.0 µs.

5.9. The DLS experiment

The nature and great sensitivity of DLS obliges the user to take extra caution when preparing the samples for analysis. Any external contaminant like dust, dirt will heavily alter the outcome of the analysis. To avoid this, samples are preventively filtered using microporous

filters. In some cases, however, samples may be sensitive to the filtering, and it is recommended to filter the solvent prior to making the solutions.

Six sets of samples, containing three different AOS (U, NP and OP) and different salt concentrations were made. The concentrations ranged from 1 to 8 % in weight of surfactant, and 1.6 to 0 % in weight of NaCl, this is summarized in table 3. All of them were made by mixing the components with water previously filtered using a 0.22 µm pore size filter.

Table 3: Summary of the concentrations used for the DLS samples. This series was made three times, one using NP AOS, another using U AOS and the last using OP AOS.

AOS (% wt.)	**Salt (% wt.)**
8	0
4	0
2	0
1	0
8	1.6
4	0.8
2	0.4
1	0.2

The DLS Malvern Zetasizer S was used. The instrument was turned on and left to equilibrate during 1 hour before the experiment started. Then, the analysis was performed using disposable cuvettes. The parameters of the system were accordingly selected to match the recipient's material and the use of water as solvent. The acquisition time and the other collection parameters relating the laser were set on automatic, and 5 analysis per sample were performed.

6. Results

6.1. Birefringence and Viscosity results

Table 4 summarizes the outcome of the birefringence and viscosity experiment. In it, a major difference between the purified surfactant (NP) and the unpurified surfactant (U) can be observed.

Table 4: Birefringence experiment results. P.S. stands for phase separation.

AOS kind	AOS conc. (% wt)	NaCl conc. (% wt)	$C_{12}OH$ conc. (% wt)	Viscosity comparison to OP AOS 10:2:1	Anisotropy
NP	10	3	1	*More viscous.*	P.S.
	10	2	1	*Similar viscosity.*	
	15	3	0	*Less viscous.*	
	15	3	1	*More viscous.*	
	20	3	0	*Same viscosity.*	
U	10	2	1	*Water-like.*	
	15	3	0	Water-like.	
	15	3	1	Similar viscosity.	
	20	3	0	Water-like.	
2F	10	2	1	Water-like.	
	15	3	0	Water-like.	
	15	3	1	More viscous.	
L	15	3	0	Water-like.	
	15	3	1	More viscous.	

Active
Inactive

The samples where the NP AOS was used showed shear-induced anisotropy while none of U AOS did. Moreover, the recorded data shows that salt is sufficient for NP AOS to show a viscosity increase, compared to the rest of the AOS samples that also require 1-dodecanol.

Unexpectedly, a difference in viscosity between the old and new purified AOS samples was noticed. For all cases with the same concentrations, old surfactant samples are more viscous than their newer counterparts.

6.2. Surface tension and CMC results

The results from the two series of dilutions were plotted in the two graphs below, figures 10 A and 10 B.

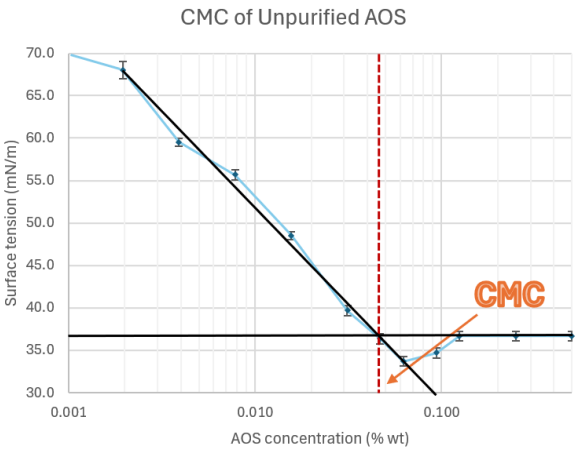

Figure 10 A: Surface tension of the New Purified AOS.

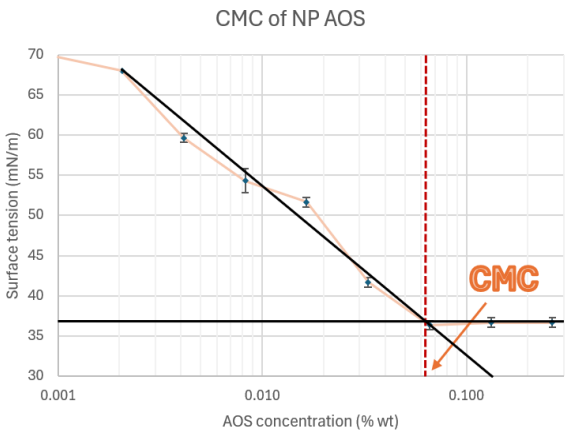

Figure 10 B: Surface tension of the unpurified AOS.

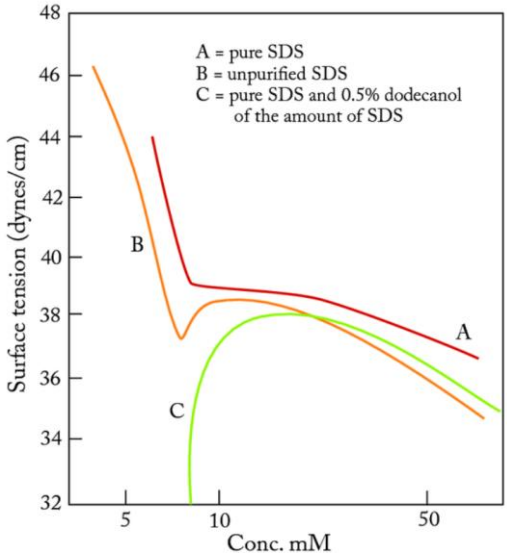

Figure 10 C: Effects on surface tension of 1-dodecano impurities in SDS. Peter H. Elworthy and Karol J. Mysels 1966.[14]

Comparing plots 10 A, 10 B and 10 C, the respective purified and unpurified versions of AOS and SDS follow similar trends in surface tension. The CMC of AOS was reached at, roughly, 0.06 % weight for the NP AOS series, and at 0.045 % mass for the U AOS series. Or at 2.2 mM and 1.6 mM, respectively, assuming a molecular weight of 275 g/mol. Also, the CMC for AOS is reached at a lower concentration than for SDS.

A different behaviour can be noticed between the samples. In NP AOS, once the CMC is achieved, the surface tension becomes constant. That does not happen in U AOS, where the surface tension shows a minimum when increasing concentration and increases after the CMC, until it flattens out. The explanation to this phenomenon is the presence of impurities with higher surface activity than the AOS, which are largely removed during the purification process.

It must be noted that calculating the CMC using the surface tension in systems containing impurities is not advised because said impurities alter the surface tension. A conductivity method could deliver a more reliable value for CMC.

6.3. Other surfactants

The corresponding study was performed on SCI and SMCT. Two series of samples of each surfactant were made following the same parameters as in the AOS series. See table 5:

Table 5: SCI and SMCT experiment samples.

Surfactant	Surfactant conc. (% wt.)	NaCl conc. (% wt.)	$C_{12}OH$ conc. (% wt.)
P.SCI	10	2	1
	15	3	0
	15	3	1
	20	3	0
SCI	10	2	1
	15	3	0
	15	3	1
P. SMCT	10	2	1
	15	3	0
	15	3	1
	20	3	0
SMCT	10	2	1
	15	3	0
	20	3	0

In all cases, at room temperature, a white dispersion is obtained. Regardless of being purified or not, the SMCT samples give rise to a liquid with similar flowability as water. On the other hand, SCI samples thicken reaching a state similar to a liquid-in-solid dispersion.

This, however, changes upon exposure to higher temperatures. At 40 ºC all the samples without 1-dodecanol changed to clear solutions with enhanced viscosity and birefringence. The most plausible explanation is that the Krafft point is reached upon increasing the temperature, allowing the surfactant to solubilize and form micelles. However, the samples with 1-dodecanol phase separated.

6.4. HPLC-ELS results

6.4.1. Pharmaceutical column

In figure 11, the chromatogram obtained from the experiment with the pharmaceutical column is found.

The chromatogram revealed that most ions in AOS are sodium. It showed that there is little difference between NP and UP, and that only trace amounts of other ions are present in the samples.

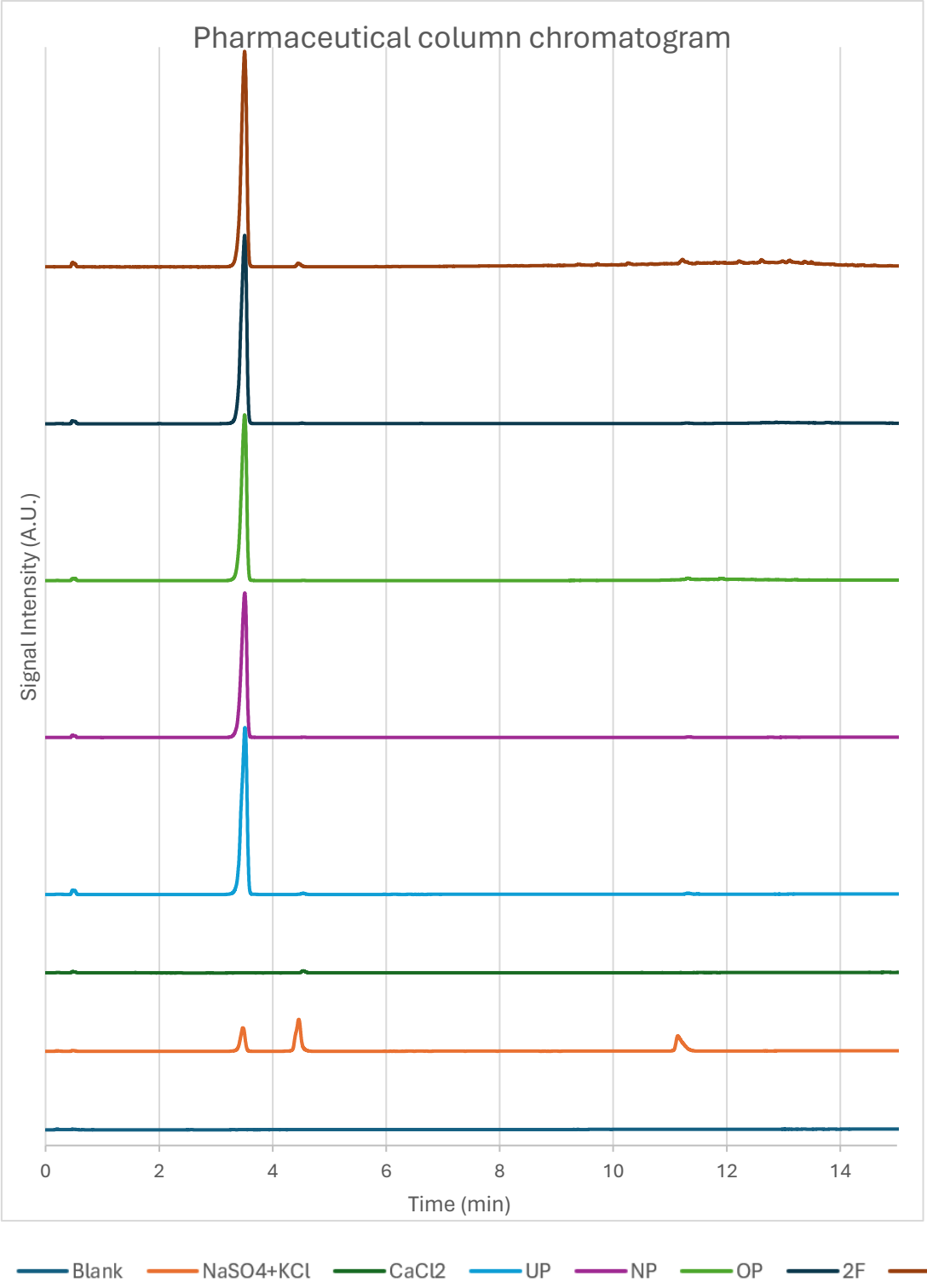

Figure 11: Chromatogram obtained from HPLC-ELS using the pharmaceutical column.

6.4.2. Surfactant column

The chromatograms resulting from the surfactant column use are found in figures 12 A, 12 B and 12 C.

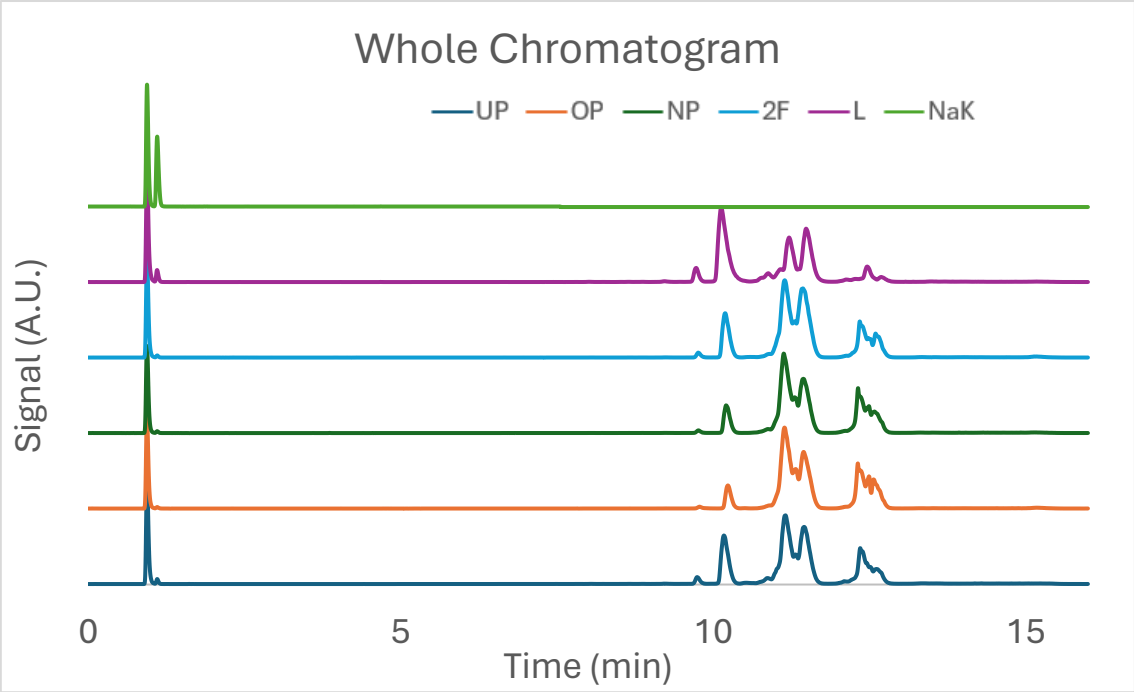

Figure 12 A: Complete chromatograms obtained from the HPLC-ELS surfactant column.

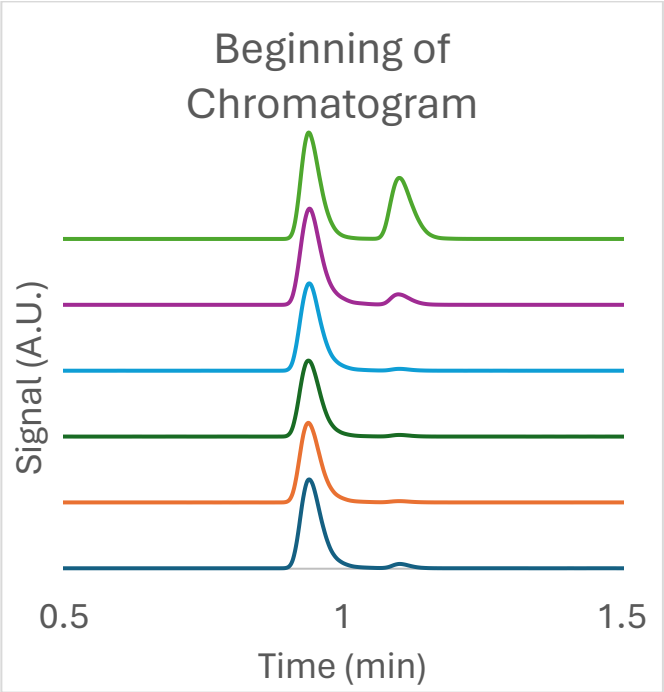

Figure 12 B: First two minutes of the chromatograms obtained from the HPLC-ELS surfactant column.

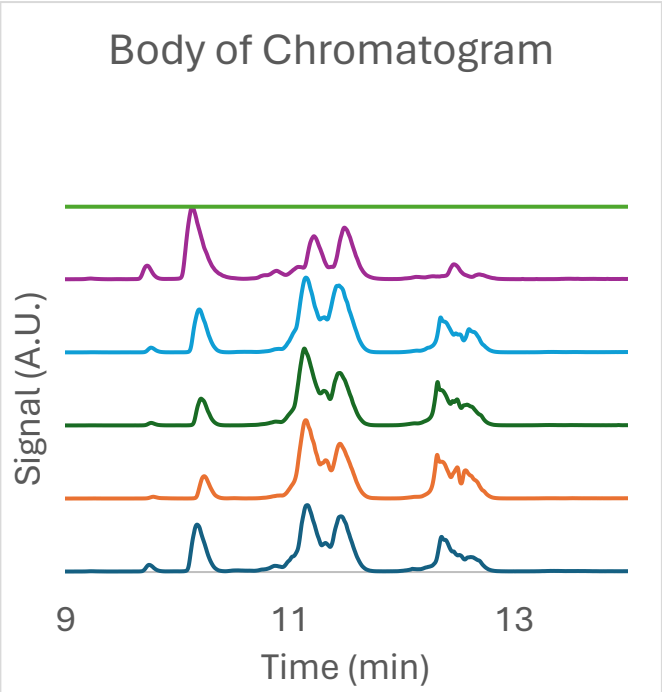

Figure 12 C: Central part of the chromatograms obtained from the HPLC-ELS surfactant column.

Following the findings with the pharmaceutical column, the first two peaks indicate little difference in salt content between the samples. Thanks to the standard of sodium sulphate and potassium chloride made, the top chromatogram. Now it is known that the peaks eluting around minute 1 relate to the salts in the system. Specifically, the first peak originated from sodium and the second peak from potassium. In the close-up figure 12 B, the potassium peak is almost non-existent for the treated samples, but it is present in L and UP surfactants.

Much more information can be extracted from the peaks between minutes 9 and 13. The two peaks eluting around minute 10 are reduced considerably in the treated versions, compared to the leftovers and the untreated version. Peaks eluting at 11 minutes do not go through a dramatic change, but their shape has been distorted. With the earlier peak getting larger in comparison to the rest of them. Lastly, the last part of the chromatogram seems to grow in comparison to the rest of the chromatogram for the purified versions of AOS. Additionally, it is almost non-existent in L. Therefore, it is safe to assume that it is the least affected by the purification process, and it either has no negative effect on building viscosity, or help it helps in the process.

6.5. HPLC-MS and MS/MS results

MS was the most valuable technique regarding the AOS content characterization. Since the same column as in ELS was used, the shape of the chromatogram is fairly similar to the ELS ones. See figure 13 A and 13 B.

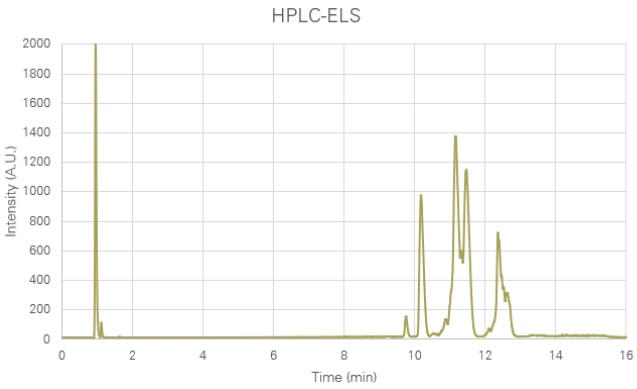

Figure 13 A: HPLC-ELS chromatogram using the surfactant column on NP AOS.

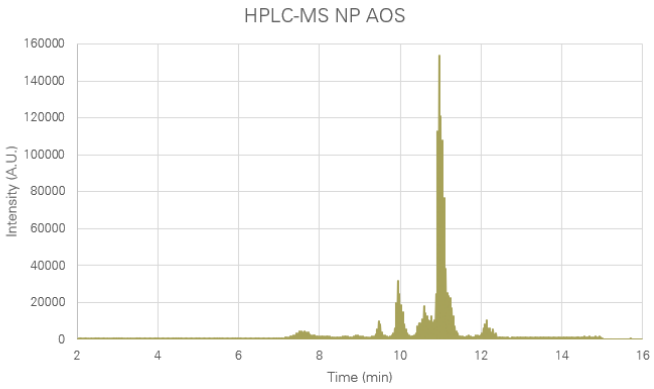

Figure 13 B: HPLC-MS chromatogram using the surfactant column on NP AOS.

In MS, excessive salt content can damage the detector, therefore, during the first two minutes of the chromatography the eluted liquid is directed into the waste. Overlooking those two minutes, it can be observed that both chromatograms that follow present the same number of peaks eluting at almost identical times. However, the relative intensities of the peaks have changed as another detector is in use.

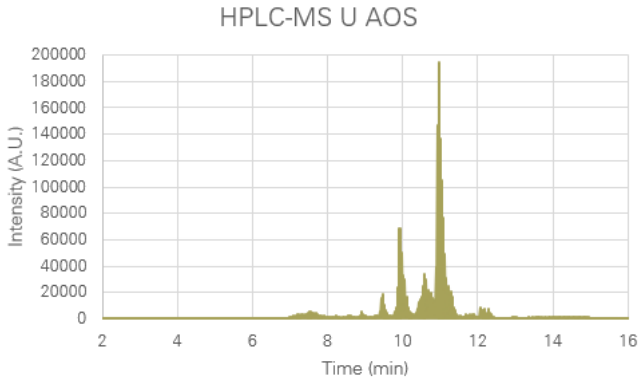

Figure 14 A: HPLC-MS chromatogram using the surfactant column on U AOS.

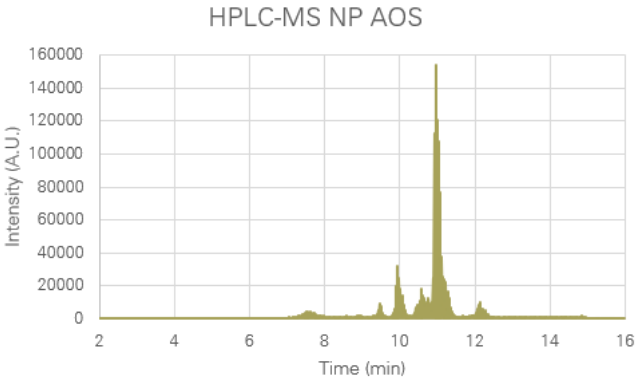

Figure 14 B: HPLC-MS chromatogram using the surfactant column on NP AOS.

The chromatograms of U AOS and NP AOS, figures 14 A and B, are similar in shape but the relative intensities of the peaks one to another have changed slightly. Specially, the peak eluting after 10 minutes now has significantly lower relative intensity.

The first MS revealed four different molar masses: 275, 293, 303 and 321, respectively. With the previous knowledge, it was hypothesized that those masses were related to two different hydrocarbon tail lengths, corresponding to surfactant molecules with either 14 or 16 carbons. It was also revealed that some molecules contained the expected double-bond, whereas the rest had an alcohol group instead. Figures 15 A and 15 B show these different structures.

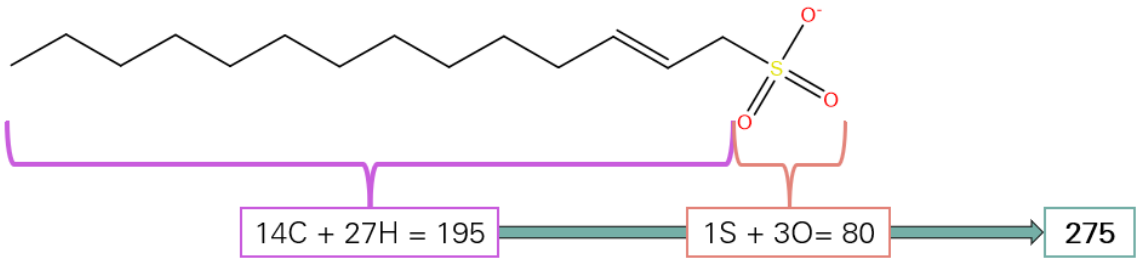

Figure 15 A: Solved structure from the MS data, full match will a 14 carbon chain AOS. With 16 carbons the mass would add up to 303.

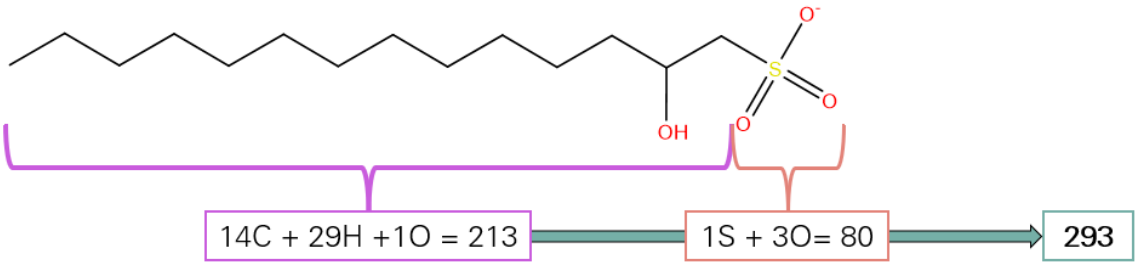

Figure 15 B: Solved structure from the MS data, with an alcohol group. With 16 carbons the mass would add up to 321. Note that the alcohol group is not strictly limited to this position.

In the doble-bond molecules, the position of the doble-bond could be guessed because the precursor is an α-olefin. However, solving the alcohol structure was not as straightforward. The next step was scanning for single different masses, see figures 16 A, B, C and D. In doing so, it was observed that for molecules with 275 g/mol two peaks were present, molecules with 293 g/mol and 321 g/mol were scattered in three peaks each, and molecules with 303 with g/mol did not draw a sharp peak in the chromatogram.

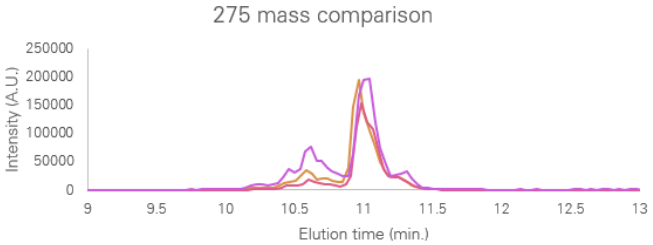

Figure 16 A: HPLC-MS chromatogram set to register 275 g/mol only.

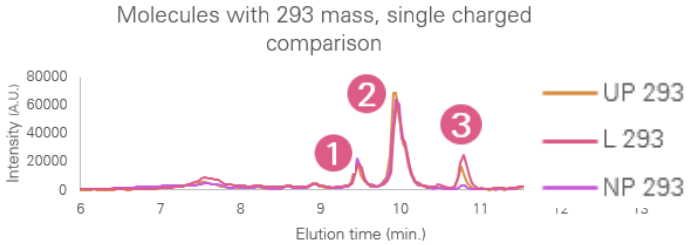

Figure 16 B: HPLC-MS chromatogram set to register 293 g/mol only. Numbers 1, 2 and 3 are used to identify each peak for the further discussion.

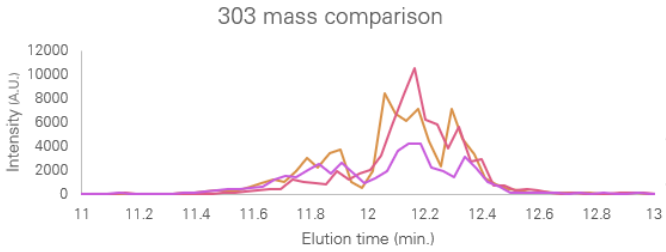

Figure 16 C: HPLC-MS chromatogram set to register molecules with 303 g/mol.

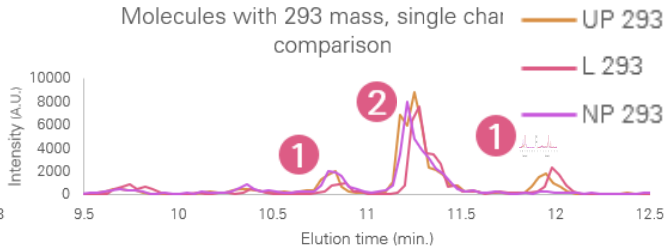

Figure 16 D: HPLC-MS chromatogram set to register molecules with 321 g/mol. Numbers 1, 2 and 3 are used to identify each peak.

The identification of the isomers was pursued using MS/MS. Exposing the molecule to a higher potential induced fragmentation, and those fragments could then be registered in the detector. In the MS/MS chromatograms for the masses 275 and 303, figures 17 A to B, only one fragment corresponding to the head group was found. For masses 293 and 321, MS/MS showed two distinct patterns depending on the peak analysed. In both cases, the first two peaks showed no fragmentation, leading to think that there is higher resistance to the fragmentation, and the last peak showed fragmentation of the head group (80 g/mol), and the head group plus a CH_2 group (95 g/mol). This last fragment can only be explained if the alcohol group is positioned on the second carbon most close to the head, like in figure 15 B, stabilizing the resulting fragment and lowering the energy required to break the molecule.

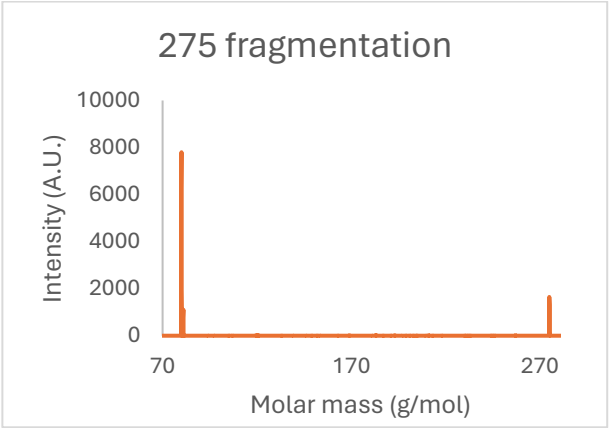

Figure 17 A: MS/MS on the 275 g/mol molecules.

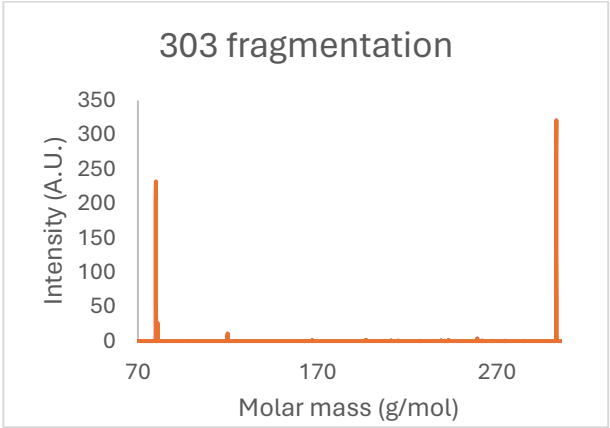

Figure 17 B: MS/MS on the 303 g/mol molecules.

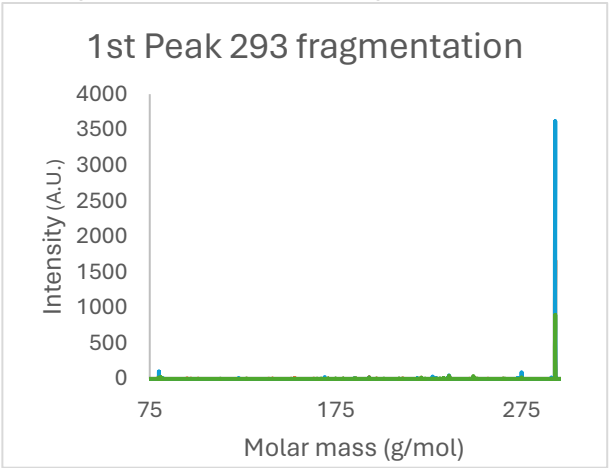

Figure 17 C: MS/MS on the first peak of 293 g/mol chromatogram.

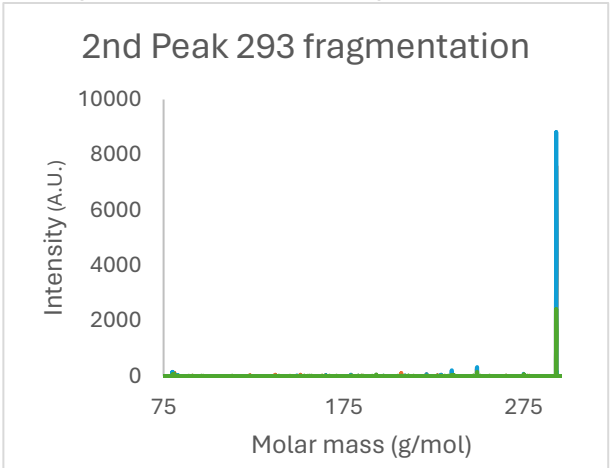

Figure 17 D: MS/MS on the second peak of 293 g/mol chromatogram.

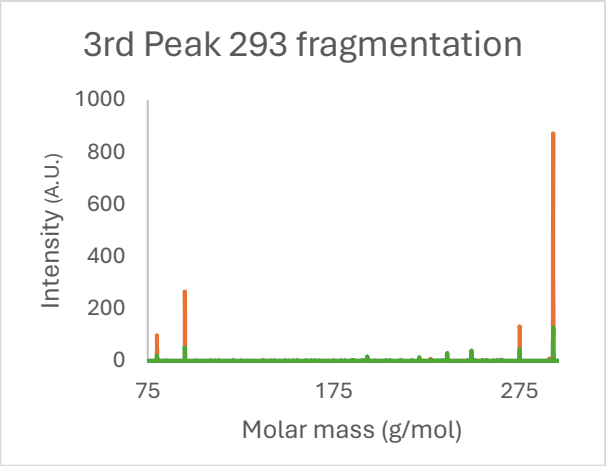

Figure 17 E: MS/MS on the third peak of the 293 g/mol chromatogram.

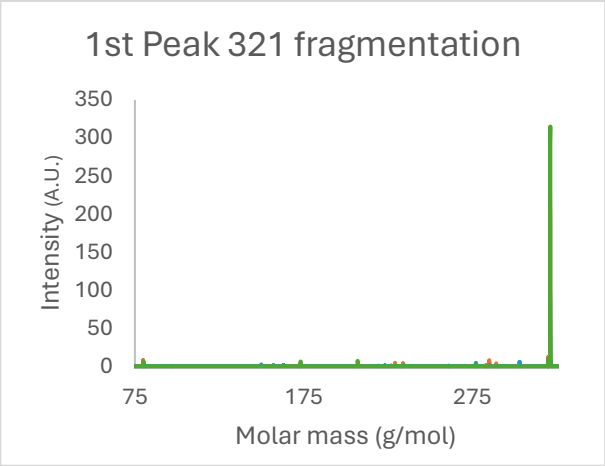

Figure 17 F: MS/MS on the first peak of the 321 g/mol chromatogram.

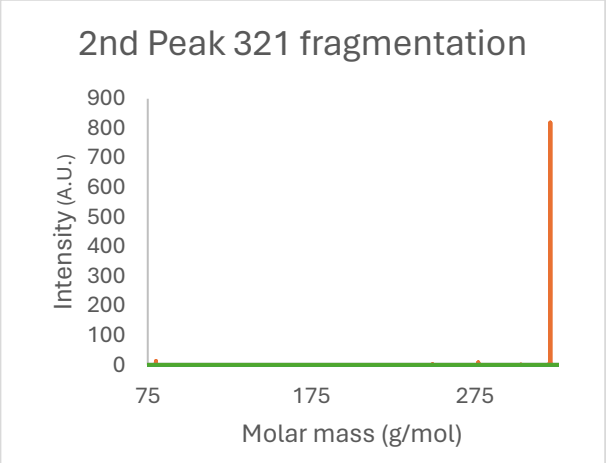

Figure 17 G: MS/MS on the second peak of the 321 g/mol chromatogram.

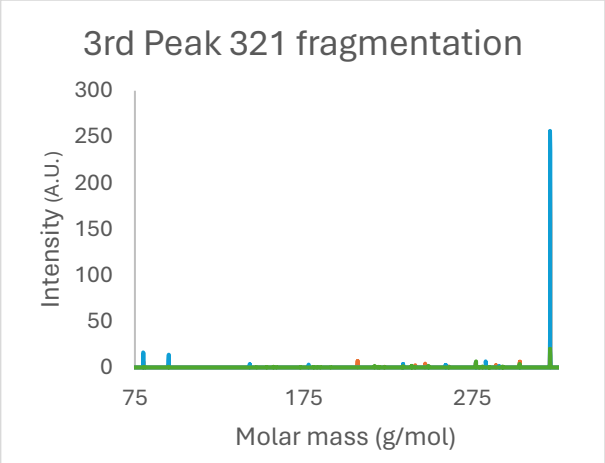

Figure 17 H: MS/MS on the third peak of the 321 g/mol chromatogram.

The rest of the isomers resisted the fragmentation, and additional information could be extracted. Nevertheless, since they show a different behaviour, the alcohol must be sitting on another atom. Moreover, if the alcohol really comes from the sultone group cleavage, then, it is most likely that alcohols sit in the carbons 3 and 4.

6.6. SAXS results

On the first data collection, the samples analysed were the same as in the birefringence experiment. No sample exceeded 20 % AOS mass concentration and they included salt, and, in some cases, 1-dodecanol. The shape of the scattering was similar for most of them. With the only significant difference being how wide or high the shape of the curve was between 0.04 Q and 0.4 Q. In figure 18, all the collected data of the first round are represented.

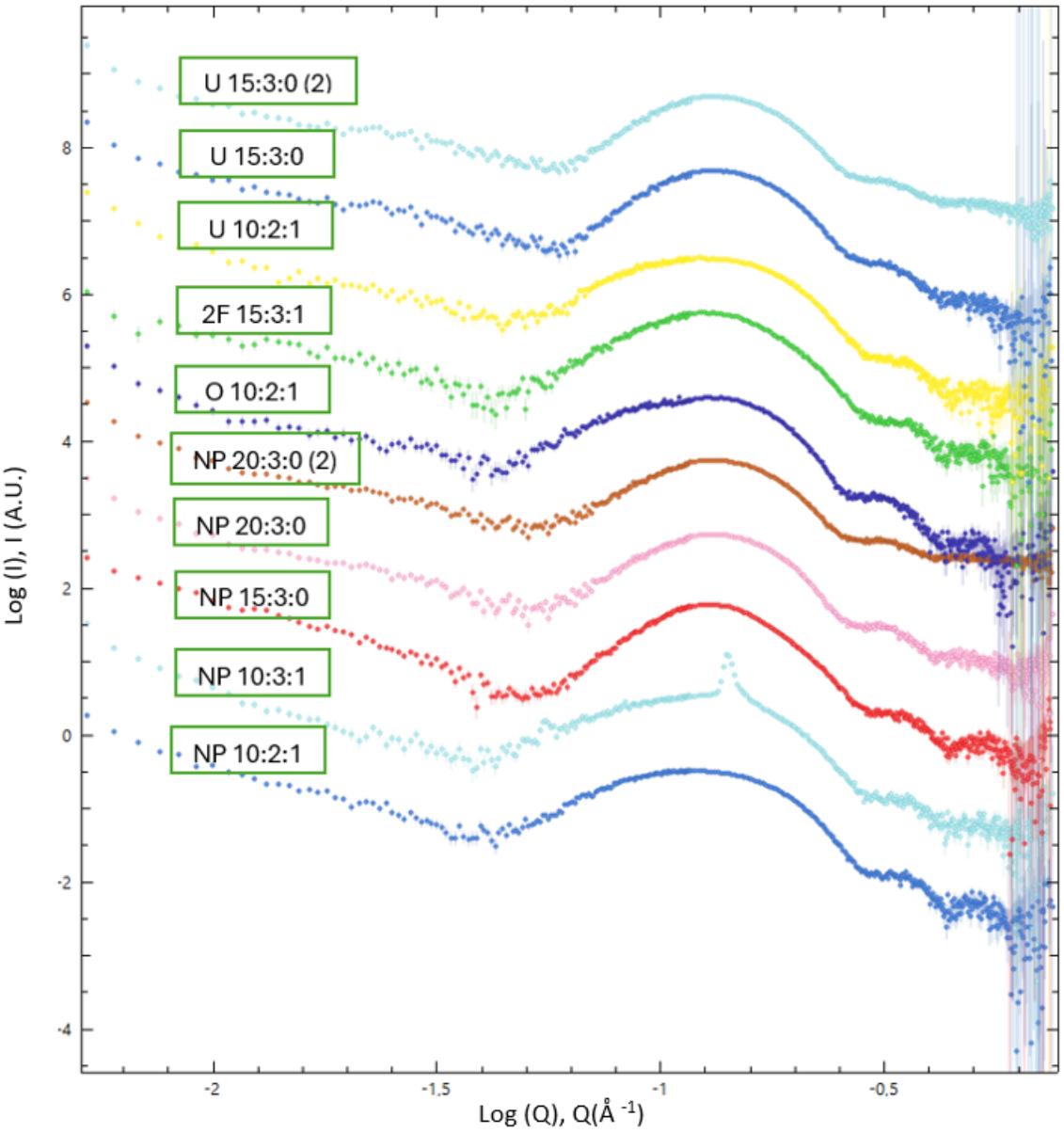

Figure 18: First SAXS results plotted using PRIMUS. Where the X axis represents, in a logarithmic scale, the q in Å $^{-1}$, and the Y axis the intensity registered in arbitrary units in logarithmic scale.

The subsequent SasView data treatment revealed an assembly that could correspond with elongated micelles or wormlike micelles, and also core shell spheres of, approximately, an internal radius of 17.4 Å and a thickness of 8.3 Å. These numbers are in agreement with the theoretical one obtained using equation 5, where it was predicted that the micelles would reach a size of 19.21 for AOS with 14 number of carbons (n_c), and 21.74 for AOS with 16 n_c.

$$l_{max} = 1.5 + 1.265 * n_c$$

Equation 5: Maximum radii of the micelle. Extracted from Kronberg, B, et al. Surface chemistry of surfactants and polymers.[1]

The difference between the experimental and theoretical value can be addressed to the thickness in SAXS including the counter-ion or the surrounding water molecules, enlarging the shell of the micelle.

In the SAXS plot, the width of the curve is indicative of a highly polydisperse sample, meaning, that the micelles in the sample appear in a variety of sizes. Additionally, the positive trend at the left of the plot suggests the presence of a greater structure or coordination.

The data did not reveal any major differences between the samples presenting an increase in viscosity and those which did not. The only outlier in the series was NP 10:3:1 which already presented phase separation. An example of the fitting done in using SasView is found in figure 19, below.

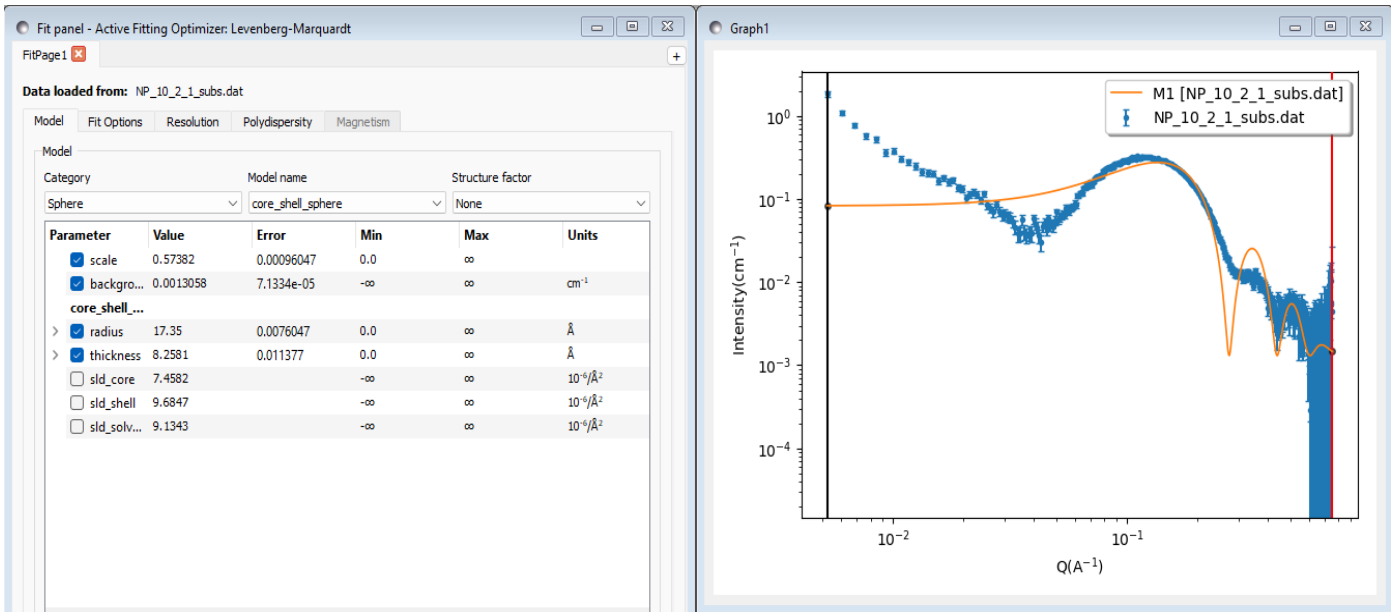

Figure 19: SasView fitting. On the left, the parameters introduced in the software to make the model, and on the right the model and the data collected in the same plot.

The second round of SAXS data collected were from gel-like or stiff heterogeneous surfactant-water samples with over 50 % AOS mass concentration, but without any other additives like in the previous collection. This time, major differences were observed between the samples. In figures 20 and 21, two plots with all the data of latter samples data are found.

The presence of well-defined peaks allowed to determine the structure and distance based on Bragg's law, table 7. The peak ratios relevant for this case are found in table 6.

Table 6: Bragg's peak ratios.[10]

Phase	Peak ratio	Peak ratio with decimals
Lamellar	1:2:3:4...	1:2:3:4...
Hexagonal	1:√3:√4:√7:√12	1:1,73:2:2,65:3,46...
Hexagonal Micellar	1:√(4/3):√(4/R²):√(4/3+1/R²)...	1:1,15...

Through the phases obtained at room temperature, and the visual inspection of the samples at different temperature, two phase diagrams were made, one for NP and one for U AOS, figure 22 A and B.

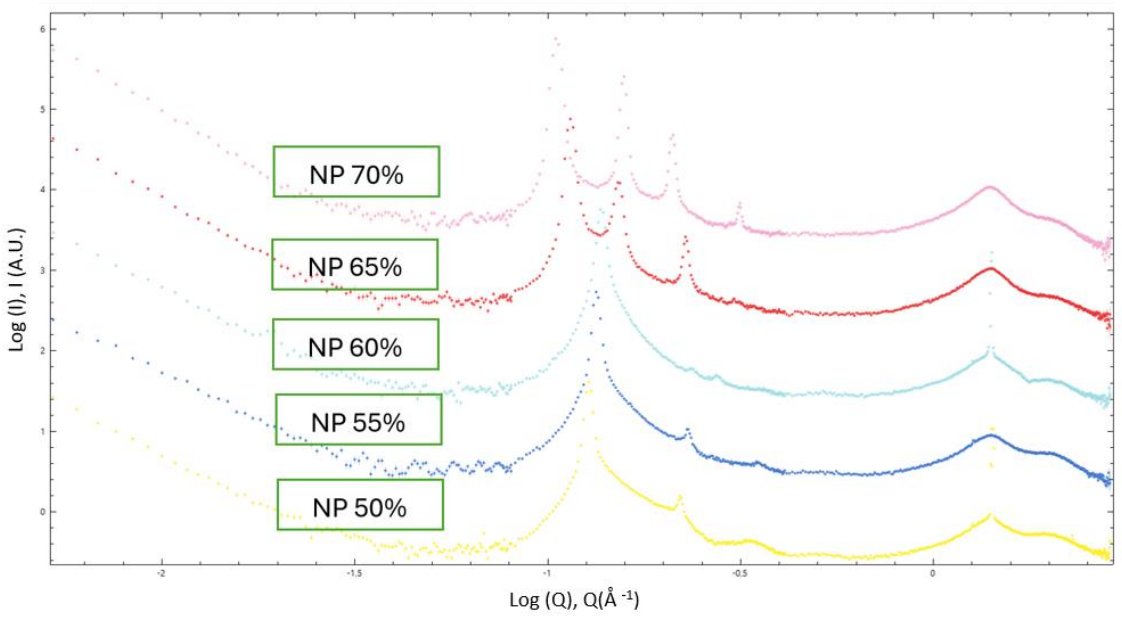

Figure 20: PRIMUS view of NP AOS samples with over 50% wt. AOS. Where the X axis represents Log(Q) for Q in Å $^{-1}$, and the Y axis the Log(I)I in arbitrary units.

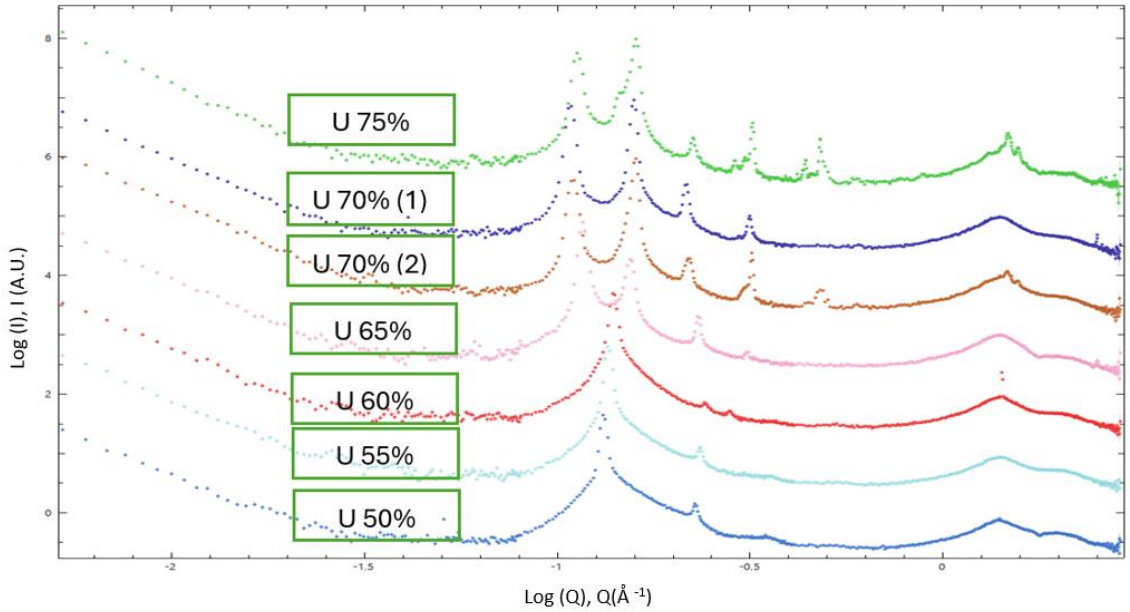

Figure 21: PRIMUS view of U AOS samples with over 50% wt. AOS.

Table 7: Mathematical treatment of the collected data using Bragg's law.

SAXS peak analysis							
Sample	**AOS % wt.**	**Peak's q**	**2*PI()/q (Å)**	**q1/qn**	**q2/qn**	**q3/qn**	**Structure**

NP	70	0.106	**59.28**	1.00			Lam. (I)
		0.158	**39.77**	1.49	1.00		Lam. (II)
		0.211	29.78	1.99	1.34	1.00	
		0.316	19.88	2.98	2.00	1.50	
NP	65	0.115	**54.64**	1.00			Lam. (I)
		0.154	**40.80**	1.34	1.00		Prob. Lam. (II)
		0.229	27.44	1.99	1.49	1.00	Lam. (I)
NP	60	0.138	**45.53**	1.00			Hex. and lam. (I)
		0.236	26.62	1.71	1.00		Hex.
		0.275	22.85	1.99	1.17	1.00	Lam. (I)
NP	55	0.134	**46.89**	1.00			Hex.
		0.232	27.08	1.73	1.00		
NP	50	0.129	**48.71**	1.00			Hex.
		0.222	28.30	1.72	1.00		
U	75	0.114	**55.12**	1.00			Lamellar (I)
		0.145	**43.33**	1.27	1.00		Lam (II)
		0.161	**39.03**	1.41	1.11	1.00	Lam(III)
		0.225	27.93	1.97	1.55	1.40	
		0.29	21.67	2.54	2.00	1.80	
		0.307	20.47	2.69	2.12	1.91	
		0.321	19.57	2.82	2.21	1.99	
		0.434	14.48	3.81	2.99	2.70	
		0.441	14.25	3.87	3.04	2.74	
		0.481	13.06	4.22	3.32	2.99	
U (TOP)	70	0.108	**58.18**	1.00			Lam.
		0.159	39.52	1.47	1.00		
		0.217	**28.95**	2.01	1.50	1.00	Lam.
		0.316	19.88	2.93	2.18	1.96	
U(BOT)	70	0.11	**57.12**	1.00			Lam.
		0.16	**39.27**	1.45	1.00		Lam.
		0.22	28.56	2.00	1.38	1.00	
		0.305	20.60	2.77	1.91	1.39	
		0.319	19.70	2.90	1.99	1.45	
U	65	0.117	**53.70**	1.00			Lam.
		0.155	**40.54**	1.32	1.00		Lam.
		0.233	26.97	1.99	1.50	1.00	
		0.313	20.07	2.68	2.02	1.34	
U	60	0.141	**44.56**	1.00			Lam.
		0.242	25.96	1.72	1.00		Hex.
		0.281	22.36	1.99	1.16		Hex. Mic?
U	55	0.137	**45.86**	1.00			Hex.
		0.236	26.62	1.72	1.00		
U	50	0.133	**47.24**	1.00			Hex.
		0.229	27.44	1.72	1.00		

The 

analysed to discern if they belong to a liqui or a crystalline phase. In future experiments, WAXS could be used to unveil their nature.

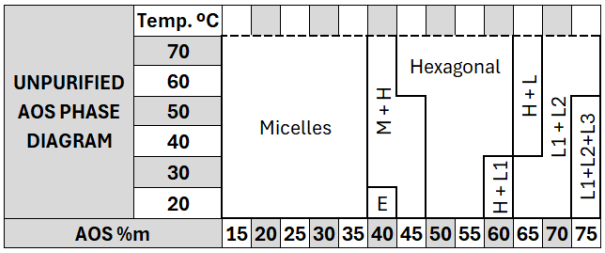

Figure 22 A: Phase diagram of U AOS. Where M stands for micelles, H for Hexagonal, L for Lamellar and E for elongated micelles.

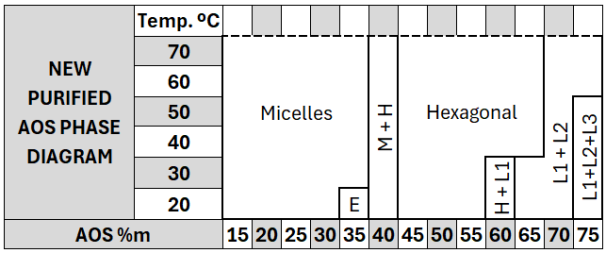

Figure 22 B: Phase diagram of NP AOS.

It can be observed that for the purified AOS, the hexagonal phase starts at a lower concentration than for the unpurified version, at room temperature. The same happens for the elongated micelles phase (E). The different phases could be confirmed utilizing other techniques such as polarized microscopy or deuterium NMR.

Notice that at 75% in weight of surfactant, three phases are found in both systems. According to the Gibbs phase rule, in a pure mixture of two compounds only two phases can coexist at equilibrium. This indicates, the presence of other species apart from AOS and water.

6.7. NMR results

The resulting ^{1}H-NMR spectra are found in figures 22 A and B, and its subsequent analysis is found on figure 23. In those, the presence of a double-bond and an alcohol was further confirmed. Additionally, the presence of the alcohol on the third carbon was confirmed.

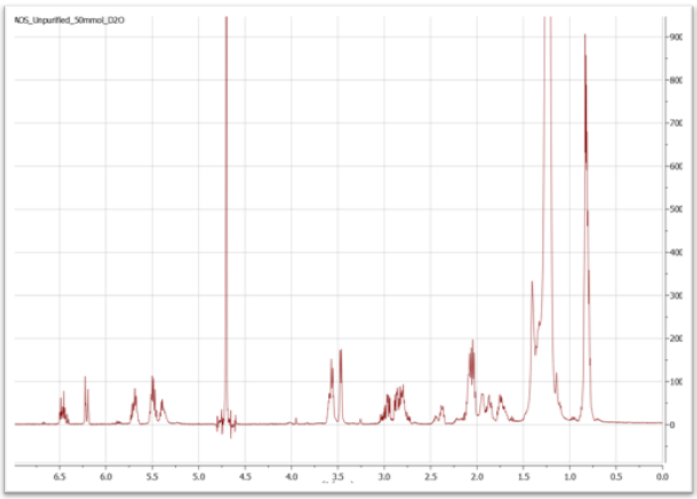
Figure 22 A: ^{1}H-NMR spectrum of U AOS.

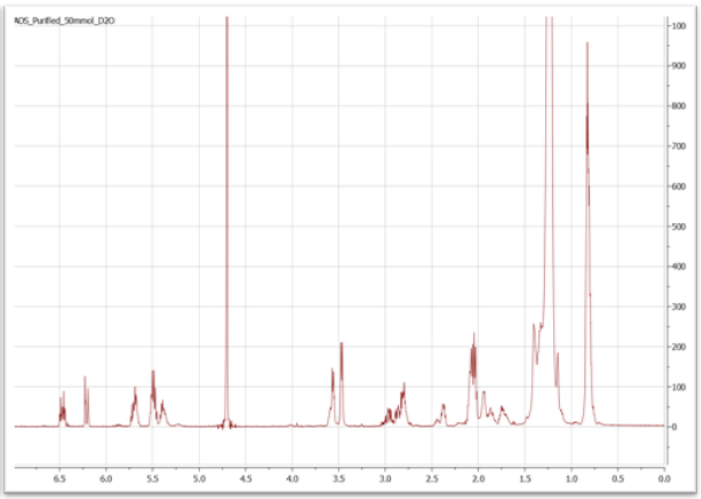
Figure 22 B: ^{1}H-NMR spectrum of NP AOS.

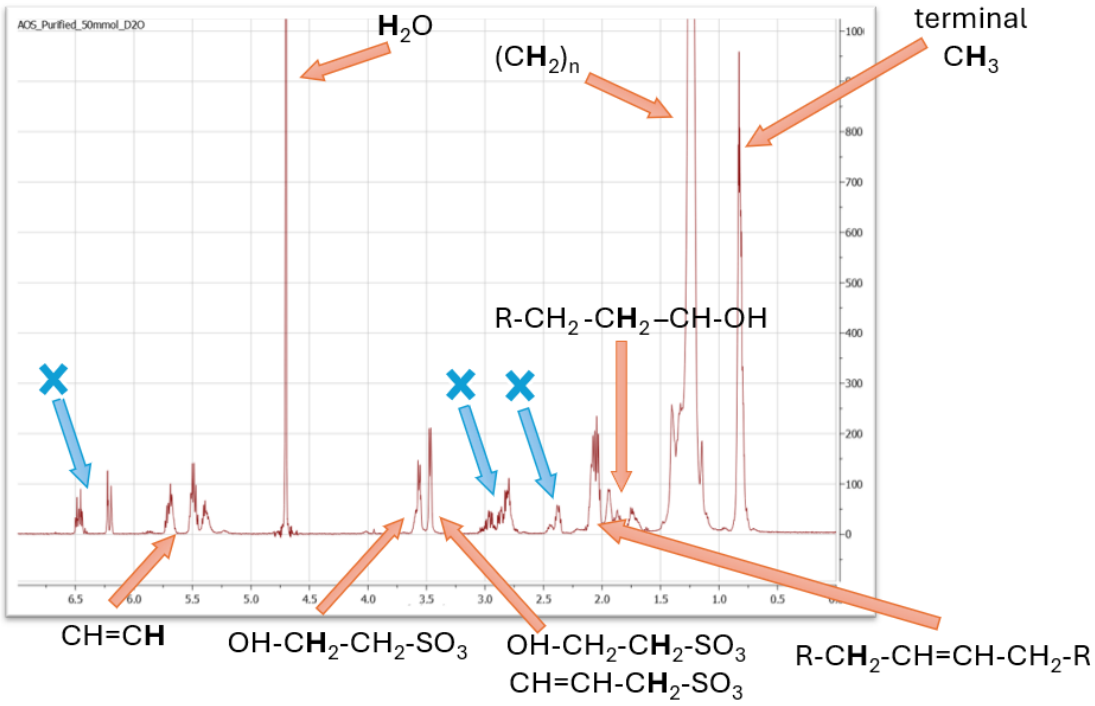

Figure 23: Resolved [1]H-NMR spectrum of NP AOS.

Not all peaks in the chromatogram could be identified, and more studies should be carried out to discover their origin. In future experiments, it would be specially interesting to discover what molecule gives rise to the peaks around 3 ppm, because those seem to differ the most between the NP and U AOS spectra.

The solved [13]C-NMR spectra is found in figure 24. Less information can be extracted from it than from the [1]H-NMR. Nevertheless, it further confirmed, again, the presence of a double bond and an alcohol group.

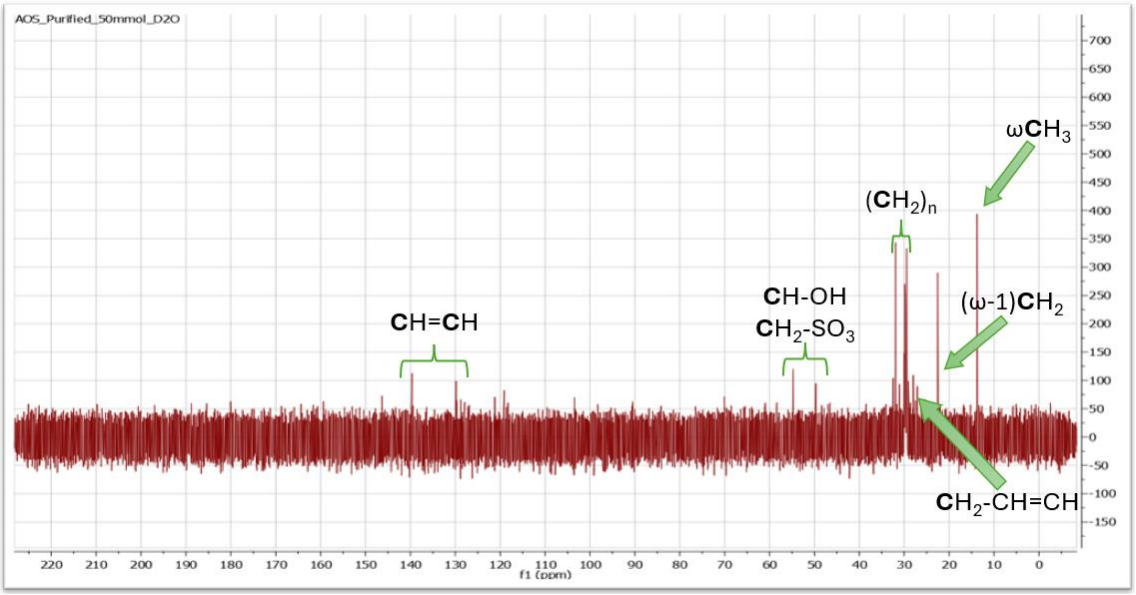

Figure 24: Solved [13]C-NMR spectra structure.

6.8. DLS results

A comparison of the correlation functions between NP AOS and NP AOS with NaCl are found below in figures 25 A and B. In those, a clear difference is spotted where the sample without additional salt experiences a bump, while the one with additional salt smoothly decreases until it reaches the bottom.

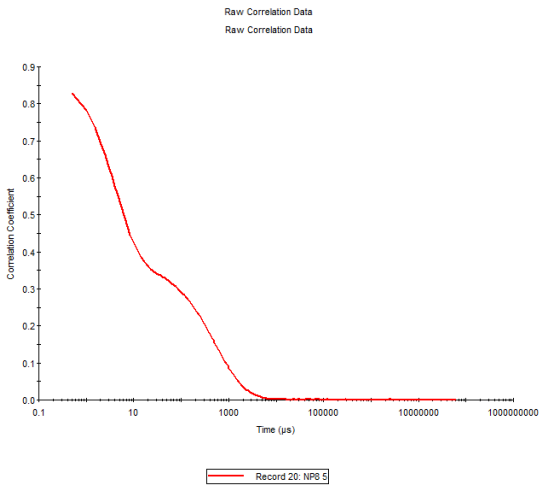

Figure 25 A: DLS's correlation function of a samples with 8% NP AOS and without additional NaCl.

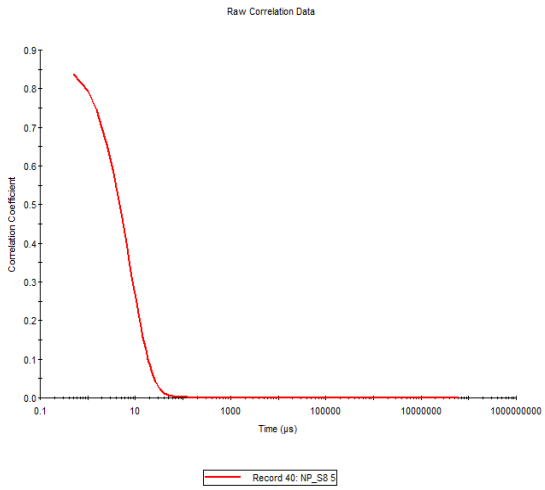

Figure 25 B: DLS's correlation function of a sample with 8% NP AOS with additional NaCl.

Due to time shortage, only the series of NP AOS and NP AOS plus NaCl were analysed. It is concluded from comparing the intensity versus size plots, figures 26 A to D, that salt prevents the formation of aggregates and homogenises the size present in the system. Additionally, incrementing the AOS concentration for the salt containing system increases the particle size, but reduces the homogeneity.

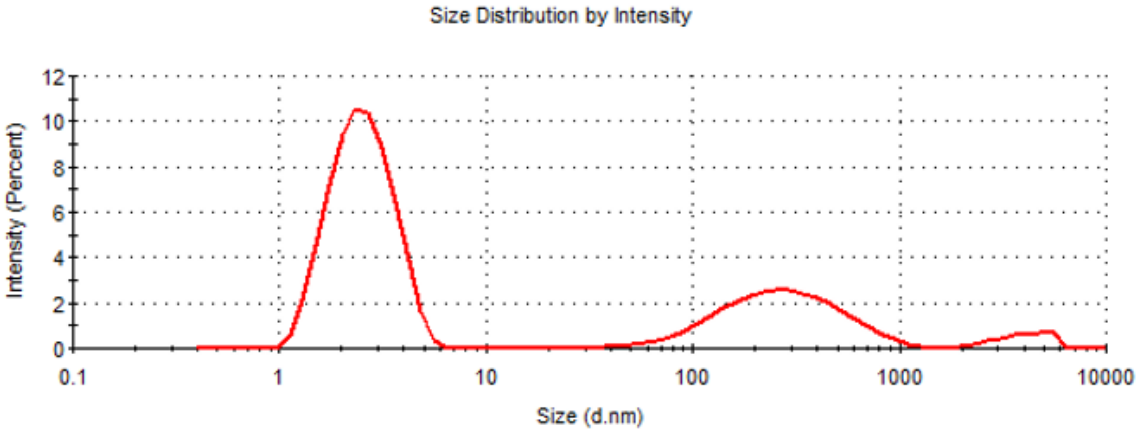

Figure 26 A: DLS Intensity vs size plot of NP AOS 1% wt., without additional salt.

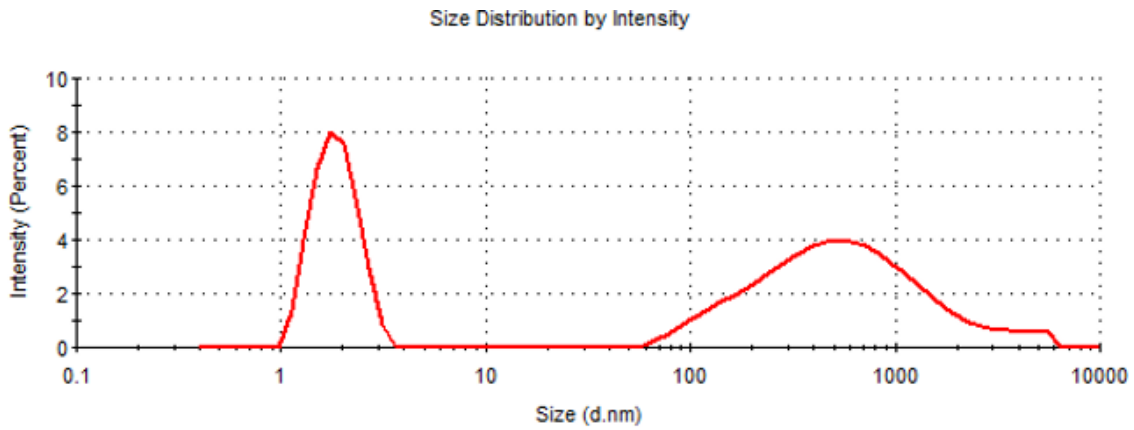

Figure 26 B: DLS Intensity vs size plot of NP AOS 8 % wt., without additional salt.

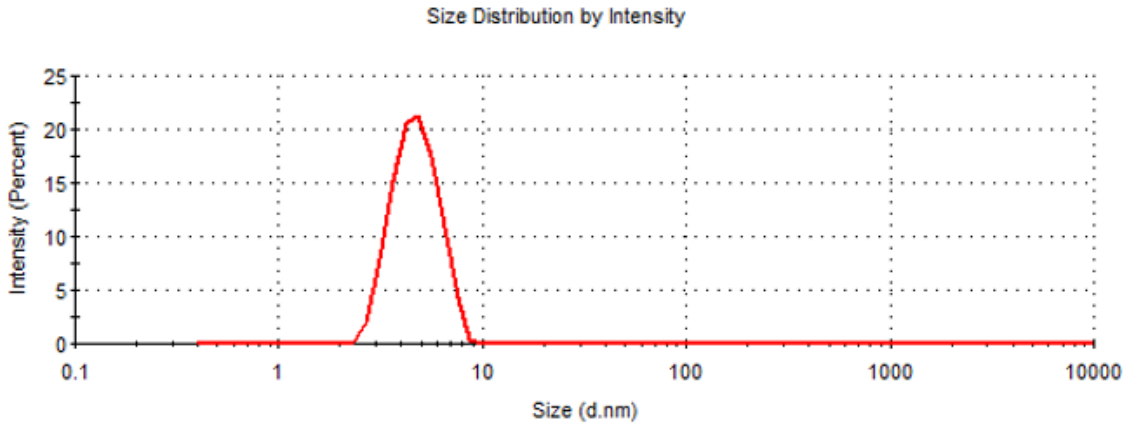

Figure 26 C: DLS Intensity vs size plot of NP AOS 1% wt. and 0.2 % wt. NaCl.

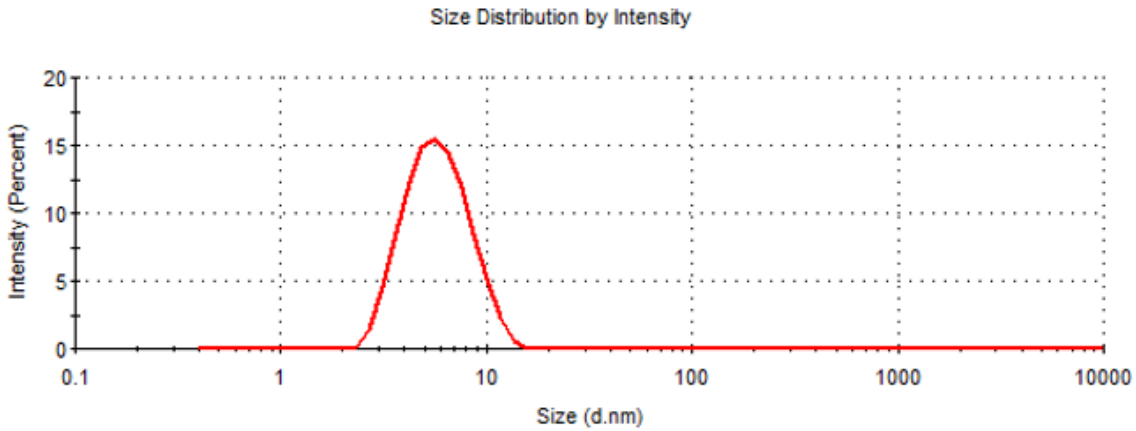

Figure 26 D: DLS Intensity vs size plot of NP AOS 8% wt. and 1.6 % NaCl.

It is not possible to correlate the presence of the bump in DLS to the ascending trend on the left side of the SAXS plot in figure18. Mainly because the concentrations used in SAXS are much higher than those used in DLS.

7. Conclusion and Discussion

Regarding the impurities of AOS, in figure 12 A, it is observed that the peaks eluting roughly at minute 10 are much lower for the purified AOS versions. Later, thanks to HPLC-MS, these peaks were revealed to belong to isomers of AOS including an alcohol group on either the third, or further carbon, counting from the sulphone group. Since the AOS with lesser concentration of these compounds had a better performance in the viscosity and birefringence experiments, it is safe to assume that they must be responsible for the challenges associated with AOS.

The mechanism that makes alcohol isomers worse at thickening the formulation can be explained through the CPP. Due to the alcohol group preferring the hydrophilic side, the head group will get bigger as the alcohol goes deeper into the aliphatic chain. Additionally, the screening effect of the counter-ion is less effective on the surfactants with the alcohol group. Consequently, the packing capacity of the surfactant, and the ability to form more elongated micelles is hindered, see figure 27.

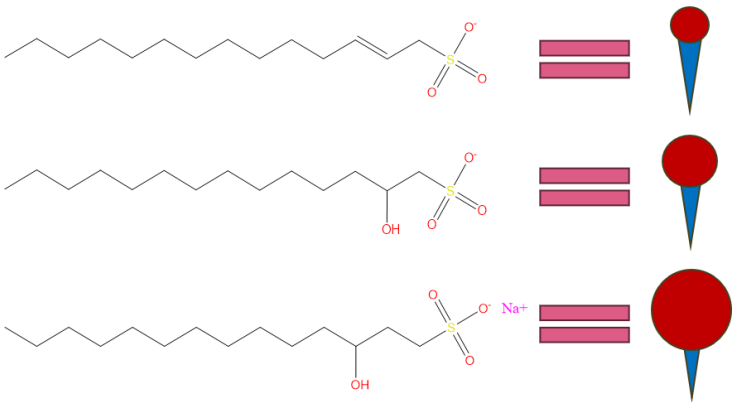

Figure 27: How the alcohol group changes the head to tail ratio of the surfactant.

In relation to the AOS characterization, more work is required. More analysis utilizing DLS, and the rheometer are on their way, but experimenting on more conditions for the system, and performing more SAXS to deliver a completely accurate phase diagram is encouraged in future research. Nevertheless, a significant achievement was accomplished and further understanding of the system was gained through this master thesis.

Upcoming experiments should also include an optimization for the purification process or a completely new processes that would eventually give rise to even better versions of AOS.

8. References

[1] Kronberg, B., Holmberg, K., & Lindman, B. (2014b). *Surface chemistry of surfactants and polymers*. John Wiley & Sons.

[2] Abbott, S. J. (2017*). Surfactant science: Principles & Practice*.

[3] Fontell, K. *Cubic phases in surfactant and surfactant-like lipid systems*. Colloid & Polymer Sci 268, 264–285 (1990). https://doi.org/10.1007/BF01490251.

[4] Haszeldine, R. N., Hyde, T., & Tait, P. J. T. (1973). Polymerization studies using modified Ziegler-Natta catalysts: 1. Polymerization of vinyl chloride. *Polymer*, *14*(5), 215–220. https://doi.org/10.1016/0032-3861(73)90048-7.

[5] Reuben, B. G., & Wittcoff, H. (1988). The SHOP process: An example of industrial creativity. *Journal of Chemical Education*, *65*(7), 605. https://doi.org/10.1021/ed065p605.

[6] Zoller, U., & Sosis, P. (2008). *Handbook of Detergents, Part f: Production*. CRC Press. Pp 131-141.

[7] Malvern Instruments WorldWide. White paper. *A basic introduction to Rheology*. 2016.

[8] Ho, C. S., Lam, C. W. K., Chan, M. H. M., Cheung, R. C. K., Law, L. K., Lit, L. C. W., Ng, K. F., Suen, M. W. M., & Tai, H. L. (2003). Electrospray ionisation mass spectrometry: principles and clinical applications. *PubMed, 24*(1), 3–12. https://pubmed.ncbi.nlm.nih.gov/18568044

[9] Bruins, A. P. (1998). Mechanistic aspects of electrospray ionization. *Journal of Chromatography a/Journal of Chromatography*, *794*(1–2), 345–357. https://doi.org/10.1016/s0021-9673(97)01110-2

[10] Hyde, Stephen T. "Identification of lyotropic liquid crystalline mesophases." *Handbook of applied surface and colloid chemistry* 2 (2001): 299-332.

[11] Carbajo, R. J., & Neira, J. L. (2013). NMR for Chemists and Biologists. In *SpringerBriefs in biochemistry and molecular biology*. https://doi.org/10.1007/978-94-007-6976-2.

[12]Hornak, J. P. (2002). Basics of NMR.

[13] Malvern (2013). Zetasizer Nano User Manual. Chapter 11.

[14] Elworthy, P. H., & Mysels, K. J. (1966). The surface tension of sodium dodecylsulfate solutions and the phase separation model of micelle formation. *Journal of Colloid and Interface Science*, 21(3), 331–347. https://doi.org/10.1016/0095-8522(66)90017-1